

## ABSTRACT

Title of Thesis: QUANTIFYING THE IMPACTS OF URBAN WIND SHELTERING ON THE BUILDING ENERGY CONSUMPTION

Saber Khoshdel Nikkho, Master of Science,  
2016

Thesis Directed By: Professor, Jelena Srebric,  
Department of Mechanical Engineering

Common building energy modeling approaches do not account for the influence of surrounding neighborhood on the energy consumption patterns. This thesis develops a framework to quantify the neighborhood impact on a building energy consumption based on the local wind flow. The airflow in the neighborhood is predicted using Computational Fluid Dynamics (CFD) in eight principal wind directions. The developed framework in this study benefits from wind multipliers to adjust the wind velocity encountering the target building. The input weather data transfers the adjusted wind velocities to the building energy model. In a case study, the CFD method is validated by comparing with on-site temperature measurements, and the building energy model is calibrated using utilities data. A comparison between using the adjusted and original weather data shows that the building energy consumption and air system heat gain decreased by 5% and 37%, respectively, while the cooling gain increased by 4% annually.

QUANTIFYING THE IMPACTS OF URBAN WIND SHELTERING ON THE  
BUILDING ENERGY CONSUMPTION

by

Saber Khoshdel Nikkho

Thesis submitted to the Faculty of the Graduate School of the  
University of Maryland, College Park, in partial fulfillment  
of the requirements for the degree of  
Master of Science  
2016

Advisory Committee:  
Professor Jelena Srebric, Chair  
Professor Reinhard Radermacher  
Research Professor Yunho Hwang

© Copyright by  
Saber Khoshdel Nikkho  
2016

## Dedication

To my grandfather

## Acknowledgements

First, I would like to thank my advisor, Dr. Jelena Srebric for her great support in this research, sharing her knowledge and expertise, and also her friendly pieces of advice to success not only in academia, but in other aspects of life.

Second, I would also like to thank Dr. Mohammad Heidarinejad for his friendship and sharing knowledge. I am proud to have Mohammad as one of my best friends who have been supporting me from the very first moment of my graduate studies in conducting research, adapting to a new environment, and helping to find answers to my many questions.

Third, I would like to extend my gratitude toward colleagues at Facilities Management, especially Dave Shaughnessy, my supervisor and friend. He was so willing to transfer his knowledge in campus buildings along with the challenges and complexities in managing energy at a community-scale.

Fourth, I want to thank all of my officemates, including Matthew, Nicholas, Itohan, Daniel, and Seon. They all contributed toward creating a productive, comfortable, cooperative, and fun atmosphere.

Fifth, I thank Stefan Gracik and Jiyong Liu for their research insights, Kai Liu for his help in coding Virtual PULSE, and Ling Chen for supporting with her radiation simulation data.

Sixth, I have to thank my parents for their love and support and teaching me how to live, which is by far my most valuable lesson learned. Also I like to thank my two brothers as they are my best role models in life.

Finally, I genuinely thank my dear Paniz for her forever love, support and kindness. This thesis would not have been possible without her encouragement.

This material is based upon work supported by the National Science Foundation under Grant EFRI-1038264 and EFRI-1452045. Any opinions, findings, and conclusions or recommendations expressed in this material are those of the author(s) and do not necessarily reflect the views of the National Science Foundation.

# Table of Contents

Dedication .....	ii
Acknowledgements .....	iii
Table of Contents .....	v
List of Tables .....	vii
List of Figures .....	viii
List of Abbreviations .....	x
Chapter 1: Introduction .....	1
Section 1.1: Motivation .....	1
Section 1.2: Energy Use and Urban Microclimate .....	2
Section 1.3: Thesis outline .....	4
Chapter 2: Literature Review .....	5
Section 2.1: Prediction of Urban Thermal Environment .....	5
Section 2.2: CFD Studies of Urban Environment .....	5
Section 2.3: Building Energy Modeling at the Neighborhood Scale .....	8
Section 2.4: The Role of Wind and Infiltration in Building Energy Use .....	12
Chapter 3: Research Objectives, Hypothesis, and Methodology .....	16
Section 3.1: Thesis objectives .....	16
Section 3.2: Research Hypothesis .....	17
Section 3.3: Research Methodology .....	17
Chapter 4: CFD and Energy Modeling Assumptions in Prediction of Urban Thermal Environment .....	19
Section 4.1: EnergyPlus Simulation Overview .....	20
4.1.1 Baseline Energy Model .....	23
4.1.2 Simplifications .....	25
4.1.3 Calibration of the Energy Model .....	29
Section 4.2: OpenFOAM CFD Background and Methods .....	31
4.2.1 Case Setup .....	35
4.2.2 Domain .....	36
4.2.3 Meshing .....	37
4.2.4 Wall Functions .....	42
Section 4.3: Method of Combining CFD and Energy Simulations .....	42
Chapter 5: Framework Validation of CFD Results for an Actual Case Study .....	44
Section 5.1: Background .....	44
Section 5.2: Data Measurement Procedure .....	45
5.2.1 Instrumentation .....	45
5.2.2 On-Site Data Collection Setup .....	46
Section 5.3: Site-Specific CFD Case .....	48
5.3.1 CFD Case Inputs .....	49
5.3.2 CFD Simulation Results .....	51
Section 5.4: CFD Simulation and Collected Data Comparison .....	51
Chapter 6: Wind-Focused CFD and Energy Studies at an Actual Neighborhood .....	56
Section 6.1: CFD Simulation and Wind Multipliers .....	57
Section 6.2: Baseline Energy Model .....	62
Section 6.3: Effect of Modified Weather Data on Specific Building Energy Use .....	65

6.3.1 Energy Model Calibration with Modified Weather Data .....	65
6.3.2 Building Energy Use Comparison with Modified Weather Data .....	71
Chapter 7: Conclusions .....	74
Section 7.1: Thesis Conclusions .....	75
Section 7.2: Directions for Future Work.....	76
Appendix A: OpenFOAM Validation Case Files .....	77
Appendix B: MATLAB Code for Wind Multipliers .....	80
Bibliography .....	81



## List of Tables

Table 1: Temperature data from two CFD turbulent simulations compared to measurement .....	52
Table 2: The wind multipliers and the affected wind direction range .....	62
Table 3: The summary of the baseline energy model inputs in Virtual PULSE.....	63
Table 4: The summary of the modifications in calibrating the energy model to monthly data.....	66
Table 5: Summary of the calibration indices .....	67

## List of Figures

Figure 1: The world's urban and rural populations, 1950-2050 (United Nations, 2014) .....	2
Figure 2: EnergyPlus Program Schematic (EnergyPlus Engineering Reference, 2014) .....	22
Figure 3: (a) A Bingmap Bird’s eye view of a neighborhood on the south of UMD campus (b) developing baseline energy model geometry for that neighborhood in Virtual PULSE.....	24
Figure 4: Typical building geometries for the automated building energy simulations (Mohammad Heidarinejad, 2016).....	26
Figure 5: Representation of buildings at four reviewed campuses using combination of the typical individual shapes.....	26
Figure 6: Energy models created by the developed framework for neighborhoods with typical shapes (Mohammad Heidarinejad, 2016) .....	27
Figure 7: Perimeter and core zones in an energy model for a building at UMD .....	27
Figure 8: (a) The electricity heat map and (b) the steam heat map for Mitchel Building at UMD campus for 2014 .....	29
Figure 9: Example of CFD domain for flow over a building neighborhood .....	36
Figure 10: SnappyHexMesh cell snap procedure (OpenFOAM: The Open Source CFD Toolbox User Guide, 2014).....	39
Figure 11: (a) Mitchell building and the surrounding neighborhood (b) the distance method mesh refinement (c) the box method mesh refinement (d) the $y^+$ value comparison on surface patches .....	41
Figure 12: (a) Satellite view and (b) Bird’s eye view of the Mitchel building and the surrounding neighborhood at the University of Maryland .....	45
Figure 13: Preparing iButton sensors for the temperature measurements, avoiding direct sunlight and rain using some aluminum foil.....	46
Figure 14: The location of the iButton temperature sensors in the experiment in July 2014 around Mitchel building on the University of Maryland campus.....	47
Figure 15: Wind rose for College Park, MD, during the experiment on June 23 <sup>rd</sup> to 27 <sup>th</sup> , 2014 using AMY data for the data-source and highcharts.com for visualization .....	48
Figure 16: (a) Mitchell building, primary, and the surrounding neighborhood, secondary buildings, STL geometry (b) the final mesh domain and the refined mesh close to the ground (c) secondary and primary buildings refined mesh (d) fine mesh on the primary building.....	49
Figure 17: The boundary conditions (a) the inlet velocity profile with maximum of 5 m/s at 10 m height and above (b) the constant heat flux resulted from Radiance solar radiation simulation .....	51
Figure 18: CFD results, the surface temperature at the time of the experiment 6/24/2014, 1 pm .....	51
Figure 19: The measured and CFD model results at four locations. Dash-lines represent iButtons minimum accuracy range.....	53

Figure 20: The surface temperature in Kelvin from CFD model along with the IR photos at the time of the experiment.....	54
Figure 21: An example of the buildings rotation in creating eight CFD cases.....	59
Figure 22: One of the wind velocity measurements at the windward facade on the two white lines .....	60
Figure 23: The measured wind velocity at the windward facades in 8 directions for Mitchell building.....	61
Figure 24: The OpenStudio model of Mitchell building as the baseline energy model .....	63
Figure 25: The monthly electricity consumption in the baseline energy model in 2014 .....	64
Figure 26: The monthly district steam consumption in the baseline energy model in 2014.....	64
Figure 27: The measured, baseline, and calibrated monthly electricity and steam comparison .....	68
Figure 28: The schedules in the calibrated energy model, the “priority schedules” are used on weekends in 2014. The 2006 is the default year in OpenStudio to define the schedule.....	70
Figure 29: Annual heat gains for Mitchell building in 2014 by adjusted and original weather data .....	72

## List of Abbreviations

EUI	Energy Utilization Index
CFD	Computational Fluid Dynamics
CVRMSE	Coefficient of Variation of the Root Mean Square Error
HVAC	Heating, Ventilation, and Air Conditioning
LES	Large Eddy Simulations
RANS	Reynolds-Averaged Navier-Stokes
NMBE	Normalized Mean Bias Error

## Nomenclature

$\alpha$	Absorptivity
$\delta$	Boundary layer thickness
$\varepsilon$	Turbulent dissipation
$\rho$	Density
$\nu$	Kinematic viscosity
$A$	Area
$h$	Convective heat transfer coefficients
$k$	Turbulent kinetic energy
$p$	Pressure
$Pr$	Prandtl number
$q$	Heat flux
$Q$	Heat transfer
$T$	Temperature
$u$	Air velocity
$V$	Volume

## Chapter 1: Introduction

The prediction of local flow quantities using Computational Fluid Dynamics (CFD) and energy simulation programs is increasingly being applied to outdoor urban areas. In both developed and developing nations, urban areas are growing rapidly, and planners are making use of every available tool to ensure this population transition is as much of a benefit as possible for both individuals and society as a whole. Recent concerns for growing global energy use have drawn interest to the effect of this urbanization trend on energy use. Dense urban areas can impact the local wind, change the pattern in which wind encounters buildings, and affect the heat gain or heat loss of the building in the long run. This thesis will develop a framework to examine the effect of local wind speeds on the building energy consumption.

### Section 1.1: Motivation

The motivation behind this thesis was mainly the point that common building energy modeling approaches do not take the neighborhood effects into account. Surrounding buildings influence on the local temperature, wind speed, and wind direction that the building experiences. While the local air temperature is dependent on a city-scale, the local wind is related to the buildings in a neighborhood-scale. Having the experience in modeling energy and airflow in campus neighborhoods shed the light on this path to see the effects of local wind speed on the building energy consumption.

Section 1.2: Energy Use and Urban Microclimate

Climate is the long-term behavior of the atmosphere in a specific area, with characteristics such as temperature, pressure, wind, precipitation, cloud cover and humidity. An urban area is an area with a high density of human created structures in comparison with the areas surrounding it. Throughout the world, the demographics are rapidly changing. The developing world, which was largely rural in the 20<sup>th</sup> century, will be nearly 60 percent urbanized by 2030 [1]. A commonly quoted statistic states that 50 percent of the world's population currently lives in urban areas. This urbanization shows a remarkable trend, considering that Cohen states that at the beginning of the 20<sup>th</sup> century, only 13 percent of the world's population was urban. In addition to this, 75 percent of people in developed nations are currently living in urban areas.

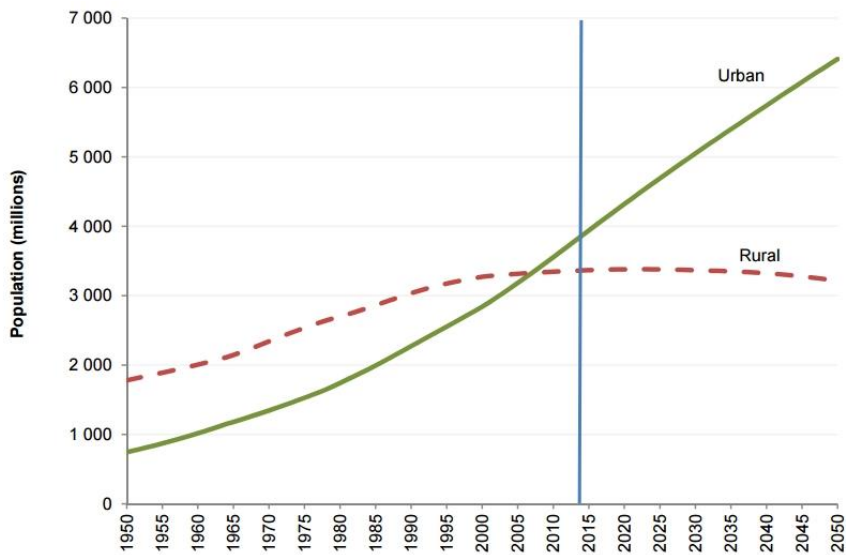


Figure 1: The world's urban and rural populations, 1950-2050 [2]

Based on United Nations report in 2014, shown in Figure 1, 54 percent of the world's population lives in urban areas, a proportion that is expected to increase to 66 percent by 2050. This drastic demographic change will surely affect energy use patterns globally. A change in energy use patterns is worthy of concern for many reasons. The world is currently heavily reliant on non-renewable fossil fuel energy sources, with greatly varying predictions as to the remaining supply. In addition to this, increasing concerns of climate change draw caution to the use of fossil fuels for energy. The EIA [3] projects that developing countries' energy use will grow at a rate of 2.2 percent compared to 0.5 percent per year for developed countries. This highlights a need to study how rapid urbanization affects the energy use in these countries.

In the U.S., buildings collectively make up 41 percent of primary energy use, according to the DOE [4]. This is an indication of an urbanized country energy use pattern, which further shows the importance in investigating the effects of urbanization on energy use, specifically building energy consumption.

Considering all the above, conducting research on the influence of the building neighborhood properties on the energy and airflow gains more importance. Urban microclimate studies try to provide methodologies to better understand the neighborhood thermal environment. Local wind speed is among one of the key parameters in this field that has important role in heat removal or heat addition to the buildings.

### Section 1.3: Thesis outline

The thesis is divided into seven chapters and one appendix. Chapter 1 serves as the background information showing the need for this topic, motivation behind the thesis, and the thesis outline. Chapter 2 provides a more in depth literature review about the use of CFD and energy models for prediction of urban thermal environment, and the role of infiltration in the energy models as one of the key parameters influenced by local wind. Chapter 3 explains the research questions grown from the research gaps, research hypothesis and methodology. Chapter 4 describes the developed framework, a detailed explanation and reasoning for the CFD and energy analysis software selected. Chapter 5 presents the validation analysis for the CFD study compared to measured environment data from the University of Maryland campus. Chapter 6 shows the implementation of the framework on the case study, creating wind multipliers in modeling airflow in the neighborhood, developing a baseline energy model, calibrating the energy model with the utilities data, and investigates the effect of wind multipliers in the calibrated energy model. Finally, Chapter 7 serves as the conclusion for the studies in this thesis, as well as recommendations for improvements and future work.



## Chapter 2: Literature Review

### Section 2.1: Prediction of Urban Thermal Environment

Buildings located in the urban environment are one of the primary contributors to the changes in thermal, airflow, and air pollution patterns in the built environment [5]. Studying urban microclimate is a key element in the design of sustainable urban neighborhoods and restoration of communities [6]. The urban modeling of neighborhoods requires solving numerically universal system of equations including airflow, temperature, and concentration of contaminants [5]. To tackle this huge system of equations, due to the computational restrictions, it is suggested to model energy and airflow at the neighborhood scale for the simulation of built environments [5]. Recently, a wide range of studies have integrated numerical solution of outdoor airflow using CFD, and energy simulation of individual buildings [7] [8] [9].

### Section 2.2: CFD Studies of Urban Environment

Outdoor airflow CFD models either use simplified arrays of buildings [10], or more detailed models representing actual neighborhoods [11] [12] [6] [13]. The simplifications included in these outdoor airflow studies determine accuracy and computation time required for the simulations. Compared to the indoor airflow simulation, the outdoor airflow simulations are computationally very intense that require consideration of additional simplifications to allow a large-scale simulation of

urban neighborhoods. The simplifications include: (1) choice of the turbulence models, (2) representation of the mesh close and far from the building, (3) consideration of the building geometry, and (4) selection of the building of interest and the surrounding buildings in the urban neighborhood.

As the outdoor airflow can greatly influence the analysis of energy consumption of buildings, there is a need for CFD analysis of actual neighborhoods [7] [11]. The numerical solution is mostly done by two turbulence models of Large Eddy Simulation (LES), or Reynolds-Averaged Navier-Stokes (RANS) [11] [12]. Although outdoor airflow CFD simulation using LES turbulence model encompasses the Atmospheric Boundary Layer (ABL) better than the airflow CFD simulation using RANS turbulence models, it does not add much accuracy to the results [14]. Moreover, RANS model is less expensive in terms of computational time [14]. Constructing a proper domain and mesh grid for the numerical solution is the main part of the CFD model. Having a sufficiently high mesh resolution in the vertical direction close to the bottom of the computational domain is essential [14]. One related parameter is the distance between the wall surfaces to the first adjacent cell to the wall, known as  $y^+$  [15] [16]. Studies suggest that if  $y^+$  in the zone of interest is in the range of 30 to 300 using standard logarithmic wall functions, then high resolution grid condition for resolving boundary layer is satisfied for most of the outdoor airflow simulation cells [11] [6] [5]. For the cells that they do not fall within the range of 30 to 300 for  $y^+$ , existing studies recommended to allow  $y^+$  up to higher values such as 1500 [17]. Existing studies modeled the urban microclimate with the high resolution

grid in the range of 0.5m to 1.0m for the zone of interest, while using a coarse resolution grid in the range of 3.0m to 8.0m for the surrounding zone [18] [5].

The CFD models are done in transient or steady state [11] [19]. The transient models are mostly used in the coupled simulation with energy simulation in short periods of time [6] [20]. Steady state models are used in the simplified coupled models, covering longer periods of simulation [7] [13]. The steady state analysis enables the model to examine outdoor airflow in different points of time in a year by the trade-off of neglecting small changes in the weather during the simulation time. At present, the unsteady analyses are mostly done in the time scale of a day up to a week [6] [10]. As there are a number of simplifications in the model, and as an intrinsic part of numerical solution, the CFD model should be validated. In actual neighborhood cases, temperature around the buildings, as a representative, is compared [21]. This comparison is done by on-site temperature measurements [11], or by infrared satellite data [6].

As a part of modeling energy and airflow in actual urban neighborhoods, there is a need to build CFD models dealing with multiple buildings. In CFD cases of the actual neighborhoods, the complexity and the scale of the geometries necessitate automated meshing. Automated meshing provides us with an easy and fast way to make a grid to solve numerical calculations for airflow around buildings. Moreover, automated meshing can facilitate the CFD process of modeling various neighborhoods in order to broaden the energy analysis to the larger scales up to cities. Automated meshing is possible in commercial software packages such as OpenFOAM.

The current study uses OpenFOAM for the CFD simulations. OpenFOAM is an open source CFD software which has been shown to be capable of providing validated results for non-isothermal urban environments [22], as well as isothermal ones [23]. Moreover, an automated mesh utility in OpenFOAM, named snappyHexMesh, gives us freedom to modify the script for meshing. Although the CFD simulations of urban neighborhoods vary in scale and complexity, snappyHexMesh is able to automatically provide a high quality mesh for the simulation domain with the ability to control effective meshing parameters effective on the quality of the mesh. The snappyHexMesh utility generates three-dimensional meshes using hexahedral and split-hexahedral automatically from triangulated surface geometries in STeroLithograpgy (STL) format. The mesh approximately conforms to the surface by iteratively refining a background mesh in the first step, snapping to surfaces in the second step, and adding mesh surface layers at last [22].

One of the main limitations in modeling the airflow in neighborhoods is that the complexities of mesh generation and the vast need for CFD computational resources have been a barrier for automatic and extensive prediction of thermal environment in neighborhoods. An exhaustive literature review showed that there has not been a fairly accurate tool for predicting atmospheric boundary layer flow in actual neighborhoods for public use other than the case studies done by researchers.

### Section 2.3: Building Energy Modeling at the Neighborhood Scale

Energy models for the building energy analysis are responsible for the energy balance in the heat generation and transfer processes. Energy models provide energy

analysis for a whole building and the Heating, Ventilating, and Air-Conditioning (HVAC) systems employed. Space-averaged indoor environmental conditions, cooling/heating load, and energy use can be obtained on an hourly or sub-hourly basis for a period of time ranging from a design day to a specific year.

While energy models make space-average indoor thermal assumptions, CFD programs, make detailed predictions of thermal comfort and indoor air quality, such as the distributions of air velocity, temperature, relative humidity, and contaminant concentrations. The distributions can be used further to determine convective heat transfer coefficients (CHTC) and thermal comfort and air quality indices such as the Predicted Mean Vote (PMV), the Percentage of People Dissatisfied (PPD) due to discomfort, the Percentage Dissatisfied (PD) due to draft, ventilation effectiveness, and the mean age of air. With the information from both energy model and CFD calculations, a designer can design an energy-efficient, thermally comfortable, and healthy building.

CFD can determine the temperature distribution and convective heat transfer coefficients. CFD can also accurately calculate natural ventilation rate driven by wind effect, stack effect, or both. However, CFD needs information from energy models as inputs, such as heating or cooling load, and wall surface temperatures. Therefore, coupling energy models with CFD is attractive to researchers [24].

There are multiple studies trying to couple energy models and CFD simulation. This coupling can be one-directional or two-directional between CFD and energy model [25]. These coupling methods are usually based on steady-state CFD simulation and unsteady state energy simulation. In one-directional coupling, at each

time step, the energy simulation program calculates surface temperatures and heat fluxes based on assumption of uniform air temperature. Then these data are used in the CFD program as the boundary conditions. Depending on the thermal boundary conditions model in the CFD program, surface temperature or heat fluxes are used to determine air temperature in the CFD domain at each time step. In the two-directional coupling, the temperature or heat fluxes at the surfaces can be exchanged between CFD and energy model in a quasi-dynamic or dynamic way. In the quasi-dynamic coupling, the converged CFD case gives adjusted surface temperature or heat fluxes to the energy model for running the next time step. However, in the dynamic coupling, the CFD and energy model should reach to a small acceptable error at each time step in terms of the surface temperatures to go the next time step. In summary, coupling brings in more accurate air and surface properties at the expense of computational time and resources. The extent of coupling being effective on the accuracy of the building energy use is pretty debatable.

The coupling is done at indoor or outdoor of buildings. The indoor coupling is mainly pursued to provide practitioners with the means to tackle problems related to poor indoor environments [26]. In the indoor coupling, energy models take in the weather and solar impact, enclosure thermal behaviors, and energy consumption, while the CFD program looks at thermal comfort (air temperature, air velocity, air humidity, and airflow turbulence), indoor air quality (contaminant concentrations) , and air distribution [27].

The outdoor coupling looks at the buildings in neighborhoods and simulates airflow around multiple buildings, from a small neighborhood to part of a city, and

energy models looks at individual building thermal behavior. The purpose of outdoor coupling is mainly to study the effect of building interactions located in urban neighborhoods and their effect on single building energy consumption [5]. Outdoor CFD has also applications in studying Urban Heat Island (UHI) [28], and outdoor thermal comfort [29].

Coupling of airflow and building energy simulation models require extensive computational time and resources. In order to provide the coupling strategies and understand the neighborhood impacts in urban areas, there are multiple studies that benefited from co-simulation rather than using dynamic coupling by definition. These studies have created the essential link between modeling airflow and energy models to take neighborhood impacts. Exterior convective heat transfer coefficients [11], infiltration rates [30], and operational Coefficient of Performance (COP) of HVAC systems [21] are some of the main parameters that are shown to be effective in this CFD and energy model linkage. For the energy models, software packages such as EnergyPlus, TRNSYS, DOE-2, eQuest, Trane Trace, and HAP are used. In this study, wind velocity and direction are the parameters that are seen in details that create the linkage between the CFD program and energy simulation.

To model multiple buildings in neighborhoods, there is a tendency to avoid coupling, while keeping the most significant links/parameters between CFD and energy models, because of the extensive need for computational resources and the unnecessary accuracy. This study tries to look for another significant parameter which is wind to build the bridge between CFD and energy models effectively and in a

simple manner. Next section will discuss the role of wind in the energy consumption of buildings and provide additional insights on this topic.

#### Section 2.4: The Role of Wind and Infiltration in Building Energy Use

The main heat transfer mechanisms in an urban neighborhood comprise of solar radiation, conduction through walls, outdoor buoyancy driven or forced convection, and evapotranspiration of greeneries. The solar radiation and conduction through walls/windows are seen in details in energy models. The convection is the one heat transfer mechanism which is not seen accurately by the energy models. The intensity of the convection is defined by  $h_c$ . The main effective parameter in the magnitude of  $h_c$  is wind.

Wind velocity and direction influence on the way thermal and velocity boundary layers come into shape in a neighborhood, and determine the type of convection from buoyancy-driven to forced one. Moreover, the geometry of the buildings and the way they are located relative to each other can influence the airflow and convection. This phenomenon can have impact on Channeling of the wind in the neighborhood, resulting in higher/lower temperatures in certain areas relative to the general flow temperature.

Air infiltration is the passage of air into a structure through joints, pores, cracks, and other openings. Such flows result from pressure differences between inside and outside air. Pressure differences in turn may be caused by the force of the wind and by difference in temperature between inside and outside air. Infiltration rates can have a significant effect on the building energy consumption [31]. The



energy loss due to infiltration was estimated to be between 6% and 9% of the total energy budget for the U.S., in a study conducted during 1980s [32]. Due to the improvements in the building insulation, the relative importance of infiltration has been increased. A more recent study shows that infiltration is responsible for 13% of the heating loads and 3% of the cooling loads for the US office buildings. Specifically, for newer buildings, infiltration is responsible for about 25% of the heating loads and 4% of the cooling loads due to the higher levels of insulation [33].

EnergyPlus contains three models, Design Flow Rate, Effective Leakage Area, and Flow Coefficient [34].

### **Infiltration by Design Flow Rate**

In this model, the user defines a design flow rate  $I_{design}$  that can be modified by temperature differences and wind speed. The basic equation [35] used to calculate infiltration with this model is:

$$Infiltration = (I_{design})(F_{Schedule})[A + B|(T_{zone} - T_{adb})| + C(WindSpeed) + D(WindSpeed^2)] \quad (1)$$

$F_{Schedule}$  is a value from user-defined schedule,  $T_{zone}$  is the zone air temperature, and  $T_{adb}$  is the outside dry-bulb temperature. The A, B, C, and D are coefficients that their values are subject to debate. The EnergyPlus defaults are 1,0,0,0 which give a constant volume flow of infiltration under all conditions. However, the more accurate range for these coefficients is studied for more accurate prediction [36].

### **Infiltration by Effective Leakage Area**

The Effective Leakage Area model is based on Sherman-Grimsrud model [37]

$$Infiltration = (F_{Schedule}) \frac{A_L}{1000} \sqrt{C_s \Delta T + C_w (WindSpeed)^2} \quad (2)$$

$A_L$  is the effective air leakage area that corresponds to at least 4 Pa pressure differential.  $C_s$  is the coefficient for stack-induced infiltration,  $\Delta T$  is the absolute temperature difference between zone air and outdoor air, and  $C_w$  is the coefficient for wind-induced infiltration.

### **Infiltration by Flow Coefficient**

Based on [38] the flow coefficient model is

$$Infiltration = (F_{Schedule}) \sqrt{(cC_s \Delta T^n)^2 + (cC_w (s * WindSpeed)^{2n})^2} \quad (3)$$

where  $c$  is the flow coefficient,  $n$  is the pressure exponent, and  $s$  is the shelter factor.

EnergyPlus assumes an average infiltration rate on the building enclosure. However, there are studies which use multi-zone and time-dependent airflow rates using software packages such as CONTAM to improve the accuracy of infiltration rates and building energy model [39]. One study has showed that time-dependent infiltration rates could increase the accuracy of energy simulations with 3% to 11% reduction in the Coefficient of Variation of the Root Mean Square Error (CVRMSE), and 2% to 11% reduction in the Normalized Mean Bias Error (NMBE) [30].

EnergyPlus uses one of the mentioned simplified models for all the wall surfaces assuming that the walls in all directions experience the same wind speed or ambient temperature. However, in urban areas with the presence of other buildings wind and temperature can vary to some extent. This thesis aims to model and measure this neighborhood effect in an actual neighborhood.

## Chapter 3: Research Objectives, Hypothesis, and Methodology

Literature review revealed that one of the main limitations in modeling the air flow in neighborhoods is that the complexities of mesh generation and the vast need for CFD computational resources. This has been a barrier in developing accurate physical models and practical tools for building energy models. Researchers have coupled CFD and energy models to represent surface and air temperatures accurately. However, exploring other parameters such as local wind which represent the neighborhood effects can help improve the prediction of urban thermal environment. Common tools in energy modeling such as EnergyPlus, use methods that include wind velocity in calculating infiltration in the buildings which is among the main contributors to heat. Accurate prediction of local wind flow sheds the light on the extent local wind affects the building energy consumption pattern.

### Section 3.1: Thesis objectives

There are three objectives in this research study, including (1) developing a framework to quantify the impact of local wind flow in urban neighborhoods using airflow modeling in OpenFOAM CFD software and EnergyPlus energy simulation, (2) validating the CFD study with on-site temperature measurements in a campus neighborhood at the University of Maryland, and (3) calibrating the target building energy model with building utility data using the adjusted weather data with local wind velocities.

### Section 3.2: Research Hypothesis

Based on the literature review, wind velocity and direction mainly affects the infiltration to the building. Moreover, in a smaller scale, it affects the heat conduction through walls by influencing the exterior convective heat transfer coefficients. Calculating local wind flow shows the variation of the wind velocity on the building facade. In other words, presence of the surrounding buildings leads to the changes in the wind flow that encounters the windward facade of a target building. Adjusting the wind velocity in the input weather data should slightly decrease the building Energy Utilization Index (EUI). However, it brings about larger changes in the building energy consumption pattern. The research hypothesis for this thesis is “urban neighborhood wind sheltering has impacts on the building energy consumption patterns of buildings located in an urban neighborhood”.

### Section 3.3: Research Methodology

The method used in this study is to use reduced-order energy and airflow modeling approach and build a framework in which the local wind is represented with the least amount of details and complexities. Using reduced-order building energy models provides an opportunity to create a baseline building energy model rapidly. Then, based on the required accuracy, the main influential parameters are revisited. The modeling approach requires numerical solution of the fluid dynamics equations in prediction of the outdoor airflow, and heat balance equations for indoor thermal environment. Final converged results from numerical solutions heavily depend on the initial or boundary conditions of the problem along with other factors such as the

quality of the grid and the right selection of the solver. Hence, validating the numerical model with the actual measurements is crucial to make sure that the model accurately represents the reality. This study uses a case study, a neighborhood located on the campus of the University of Maryland, to validate the CFD simulation and also calibrate the target building energy model with the utilities data.

The urban microclimate sheltering, which is the topic of this thesis, is about that fact that the local wind flow can vary greatly relative to the incoming wind flow. The goal is to represent this variation and investigate the effect of this variation in the building energy consumption pattern. As a result, this framework requires the following steps:

1. Creating CFD airflow models of a neighborhood with incoming wind velocity of 1 m/s, blowing from eight main principal directions
2. Measuring wind velocity encountering the target building in the neighborhood at 10m height, 5m away from the windward facade in eight CFD cases
3. Generating wind multipliers based on the average measured wind velocity for the eight principal wind directions
4. Adjusting the wind velocity in the energy model input weather data by the calculated wind multipliers
5. Comparing the energy model simulations with the adjusted and original weather data

## Chapter 4: CFD and Energy Modeling Assumptions in Prediction of Urban Thermal Environment

Urban thermal environments are complicated systems of many physical phenomena occurring simultaneously. The resolution and the complexity of the model determine the computation times for computer models. Tradeoffs must be made in order to obtain a balance between computational time and accuracy. The previous chapter described several methods for handling thermal boundary conditions in urban environments, all of which varied in implementation difficulty, and model complexity. Choices for CFD models were presented as well, especially turbulence modeling.

For this study, OpenFOAM has been used as the software library for running CFD simulations. OpenFOAM is an attractive choice since it is an open source and free software license [40]. The source code is readily available and easily modifiable. The simulations in this thesis can be used as a guide for developing a specialized urban thermal environment simulator that communicates with OpenFOAM. OpenFOAM is beginning to receive more attention in the study of urban environments as well, due to the advantages of the open source model and accuracy similar to expensive commercial codes [41] [22]. The simulation use RANS turbulence modeling and a study of the effects of different models is included in a later chapter.

For the thermal boundary conditions, an energy modeling approach, as outlined in Chapter 2, is chosen. The energy modeling software package selected in EnergyPlus. Energy modeling programs are widely used in the building design

industry to help the design and also estimate the building energy use. The work in this study can present a greater impact to the design industry if it uses software compatible with it. EnergyPlus, like OpenFOAM has a free and open source software license [42].

This chapter reviews the assumptions and simplifications used in both EnergyPlus and OpenFOAM to conduct the urban thermal environment simulations. As both EnergyPlus and OpenFOAM are nontrivial in case setup, a contribution of this thesis is in explaining the methodology used to create urban thermal environment. In the later chapter, a validation of this framework is provided through an experiment.

#### Section 4.1: EnergyPlus Simulation Overview

Energy balance equations for room air and surface heat transfer are two essential equations solved by many energy simulation programs, including EnergyPlus. The energy balance equation for room air is

$$\sum_{i=1}^N q_{i,c} A_i + Q_{other} - Q_{heat\_extraction} = \frac{\rho V_{room} c_p \Delta T}{\Delta t} \quad (4)$$

where  $\sum_{i=1}^N q_{i,c} A_i$  is the convective heat transfer from enclosure surfaces to room air,  $q_{i,c}$  is the convective flux from surface  $i$ ,  $N$  is the number of enclosure surfaces,  $A_i$  is the area of surface  $i$ ,  $Q_{other}$  is the heat gains from lights, people, appliances, infiltration, etc.,  $Q_{heat\_extraction}$  is the heat extraction rate of the room,  $\rho V_{room} c_p \Delta T / \Delta t$  is the energy change in room air.  $\rho$  is the air density,  $V_{room}$  is the



room volume,  $C_p$  is the specific heat of air,  $\Delta T$  is the temperature change of room air, and  $\Delta t$  is the sampling time interval, normally 1 h [43].

The heat extraction rate is the same as the cooling/heating load when the room air temperature is maintained as constant ( $\Delta T=0$ ). The energy balance equation for a surface (wall/window) can be written as

$$q_i + q_{ir} = \sum_{k=1}^N q_{ik} + q_{i,c} \quad (5)$$

where  $q_i$  is the conductive heat flux on surface i,  $q_{ir}$  is the radiative heat flux from internal heat sources and solar radiation, and  $q_{ik}$  is radiative heat flux from surface i to surface k.

The  $q_i$  can be determined by transfer functions, by weighting factors, or by solutions of the discretized heat conduction equation for the enclosure surface using the finite-difference method. The radiative heat flux is

$$q_{ik} = h_{ik,r}(T_i - T_k) \quad (6)$$

where  $h_{ik,r}$  is the linearized radiative heat transfer coefficient between surfaces i and k,  $T_i$  is the temperature of interior surface i, and  $T_k$  is the temperature of interior surface k, and

$$q_{i,c} = h_c(T_i - T_{room}) \quad (7)$$

where  $h_c$  is the convective heat transfer coefficient and  $T_{room}$  is the room air temperature. The convective heat transfer coefficient,  $h_c$ , is unknown. Most energy programs estimate  $h_c$  by empirical equations or as a constant. If the room air temperature,  $T_{room}$ , is assumed to be uniform and known, the interior surface temperatures,  $T_i$ , can be determined by simultaneously solving Eq. (5). Space cooling or heating load can then be determined from Eq.(4). Thereafter, the coil load is determined from the heat extraction rate and the corresponding air handling processes and HVAC system selected. With a plant model and hour-by-hour calculation of the coil load, the energy consumption of the HVAC system for a building can be determined. It is obvious that the interior/exterior convective heat transfer from enclosures is the explicit linkage between room air and surface energy balance equations. Its accuracy will directly affect the energy calculated. In Figure 2: EnergyPlus Program Schematic the EnergyPlus schematic is shown. EnergyPlus comprises of many modules and programs that work together to calculate the energy required for heating and cooling using a variety of systems and energy sources.

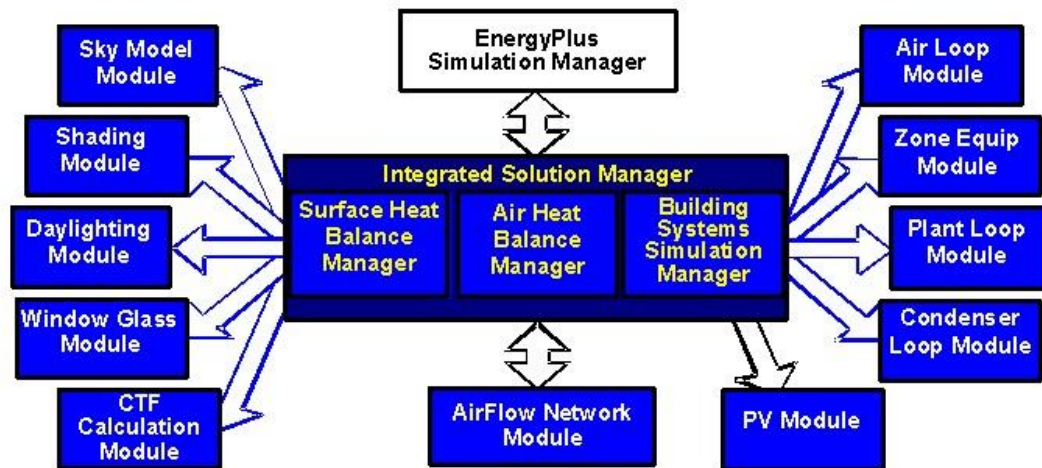


Figure 2: EnergyPlus Program Schematic [34]

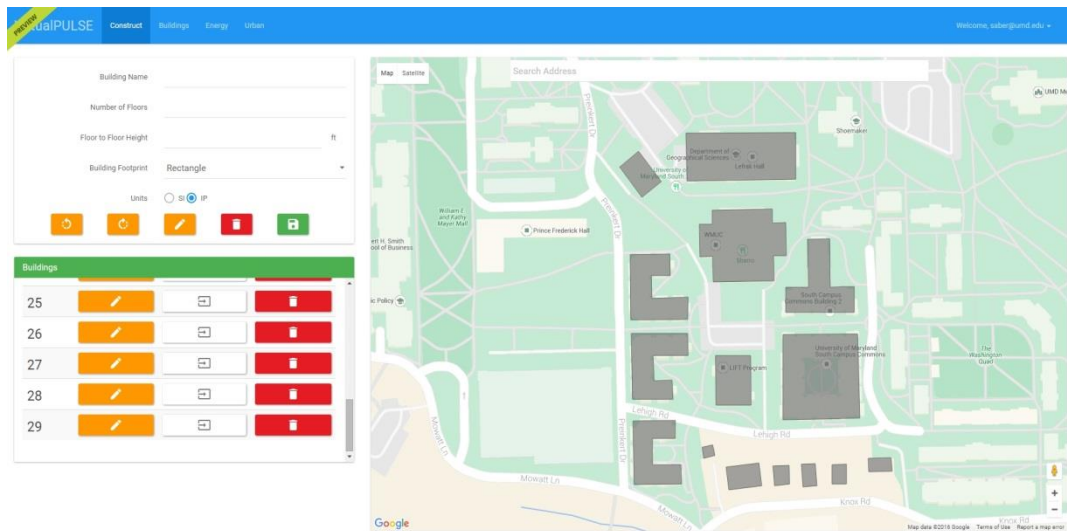
#### 4.1.1 Baseline Energy Model

Energy modeling of buildings has traditionally been exceptionally time consuming and cumbersome. Oftentimes, it takes an experienced designer days or even weeks to develop a reliable energy model. Buildings are complex, and software to model its geometry and energy demands is limited. Current software solutions lack either a user friendly front end interface or a proven back end engine. By simplifying the building input process, the user interface, and the access to such software, energy simulations reach a wider audience and empower modelers to capture even the combined effect of multiple buildings. Virtual PULSE is a new web application that allows users to simulate buildings energy and airflow [44]. The tool encapsulates an online web interface with building specification fields, geometry importing, 3D visualization, EnergyPlus simulation engine or outputs, and computational fluid dynamics airflow analyses in urban neighborhoods. In Virtual PULSE, user draws a simple footprint of the building on the GoogleMaps using standard shapes such as rectangles and T-shape footprints. Then the user enters number of floors and floor to floor height and Virtual PULSE creates a 3D simplified geometry. Based on the type of the building, Virtual PULSE creates an EnergyPlus model that has all the features such as default construction, mechanical systems, schedules, and temperature setpoints. Without getting into details, Virtual PULSE creates a simplified model that simulates your target building energy use. The user can modify the default parameters in Virtual PULSE or download an OpenStudio model (OSM) or EnergyPlus IDF file and work extensively on the model [44].

Virtual PULSE aims to provide the CFD section for advanced users modeling airflow in neighborhoods created by the simplified, standard shapes. The CFD section, captures Radiance outputs as surface heat fluxes resulted from solar radiation, then automatically creates a domain, generates a mesh based on the size of the domain and runs a CFD simulation and provides the outputs. The outputs are temperature, velocity, CHTCs, and pressure coefficients in the domain.



(a)



(b)

Figure 3: (a) A Bingmap Bird's eye view of a neighborhood on the south of UMD campus (b) developing baseline energy model geometry for that neighborhood in Virtual PULSE

This study has used the energy modeling section of the Virtual PULSE for creating the baseline energy models of the target buildings. Then the model has gone through multiple modifications and data calibration to make sure that it meets the accuracy suggested by ASHRAE Guideline 14 [45].

#### 4.1.2 Simplifications

The approach in this thesis is to reduce the details in the baseline energy model as much as possible. Simplifications in the energy models allow us to concentrate on new emerging properties [5]. These simplified models can then go through the sensitivity analysis to see the magnitude of the influence from main parameters and revisit and modify the most influential ones in the model. Through this process of tweaking the main parameters, the simplified models can reach to calibration. In the end, we have simplified models representing the reality to a good extent which have details for just some specific parameters. Here are the main simplifications in my EnergyPlus model.

##### **Use of standard shapes**

There are standard shapes used in the reduced-order models with simplified details of the building facades shown in the figure below. The typical shapes below can be used individually or by combining multiple of them attached together. These reduced-order geometries are available in Virtual PULSE. Based on a recent study on the shapes of the buildings on four different campuses, including University of Maryland (UMD), The Pennsylvania State University (Penn State), Harvard, and Portland State University, typical shapes allow representations of more than 80% of the buildings using reduced-order models [46] [47].

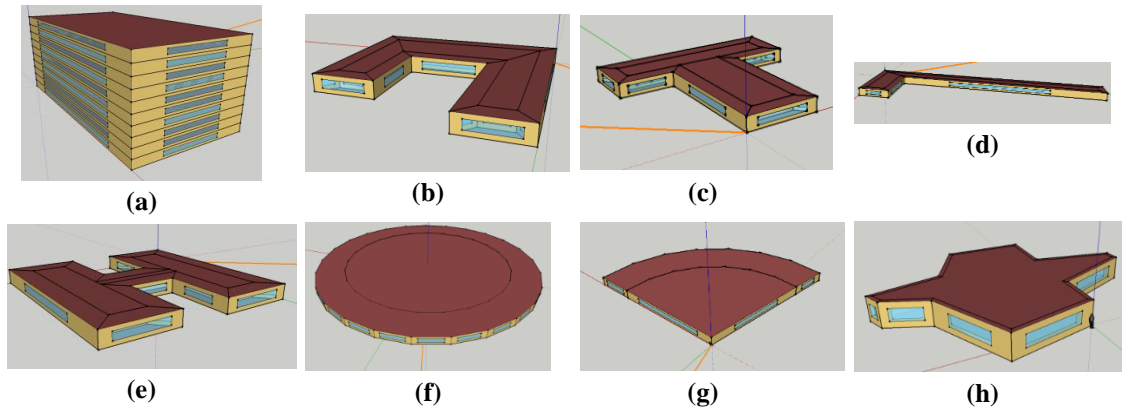


Figure 4: Typical building geometries for the automated building energy simulations [46]

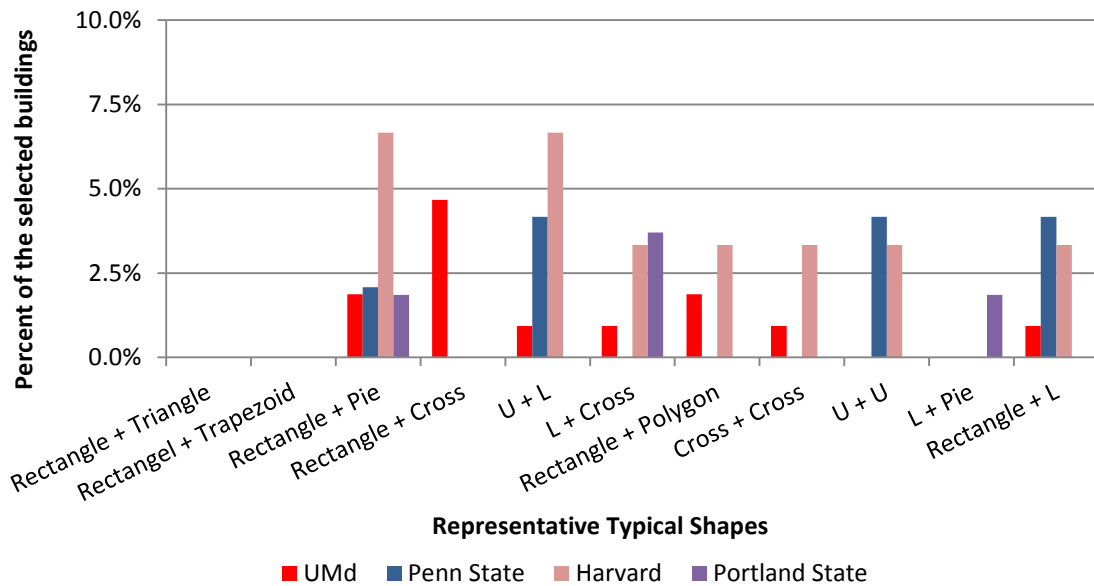


Figure 5: Representation of buildings at four reviewed campuses using combination of the typical individual shapes

### Simplification in fenestration

According to the same approach simplifying the shape of the buildings and see them in standard shapes, there are other architectural simplifications. One important architectural element is the fenestration that is simplified. Windows are seen as strips around the building facade. Each strip represents the windows of one floor. The size of the strip of windows is calculated based on the Window-to-Wall

Ratio (WWR). Figure below illustrates the developed energy models for two case studies, which represent two urban neighborhoods from University of Maryland and Pennsylvania State University.

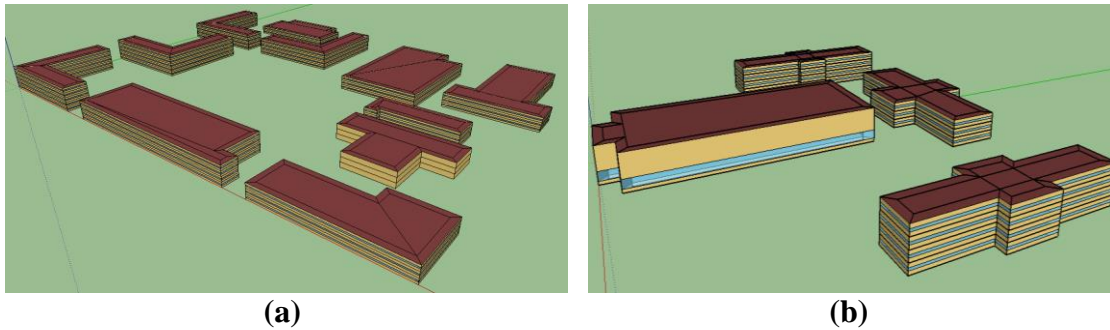


Figure 6: Energy models created by the developed framework for neighborhoods with typical shapes [46]

### Perimeter and core zoning

The interior details and complexities are not usually seen in the reduced-order energy models. Instead, interior spaces are modeled into perimeter and core zones. The size of the perimeter and core spaces is estimated based on a perimeter zone depth value. Although the perimeter spaces are the only spaces directly get the solar radiation, the inter-zone heat transfer and airflow are seen in the EnergyPlus. In the figure below, you can see the perimeter and core zones of the energy model created

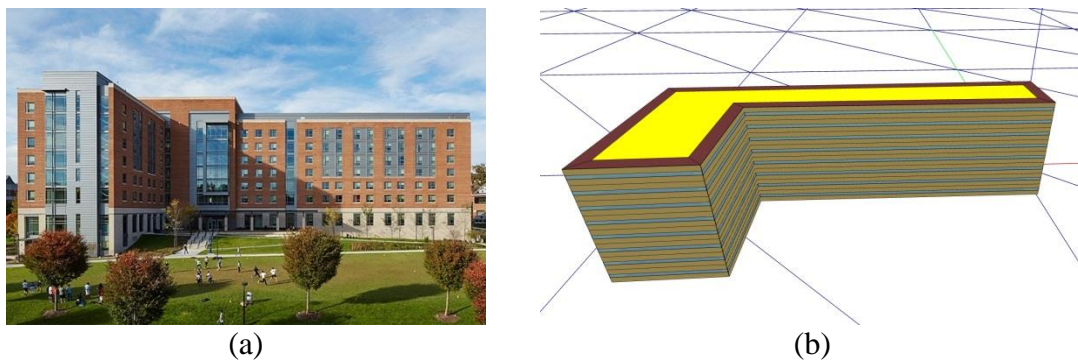


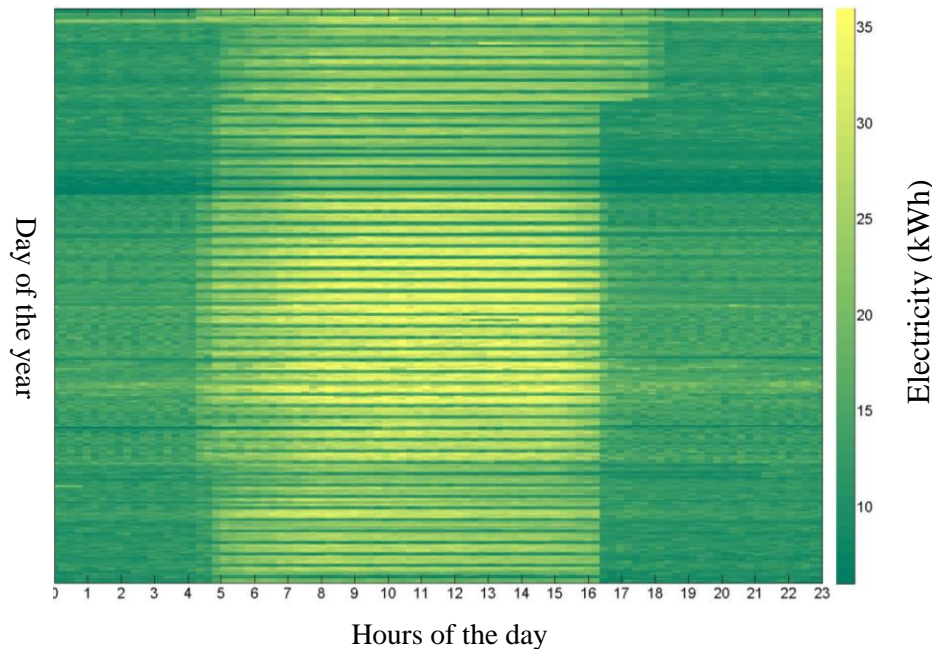
Figure 7: Perimeter and core zones in an energy model for a building at UMD



using Virtual PULSE for a building located on the campus of University of Maryland.

### Estimated schedules

The schedules for cooling, heating, occupancy, lighting, equipment and other thermal loads are very important in modeling the building energy consumption. Getting this data through thorough auditing, and control systems require multiple access permissions. Moreover, it is quite common to see occupants overriding the control and schedules during the year. One easy solution to this problem is to use heat maps of the utilities such as electricity and natural gas. Heat maps illustrate the daily energy intensity throughout the year in a compact visual format which greatly helps estimating the thermal load schedules. Usually, the electricity heat maps have higher resolution relative to natural gas or steam heat maps. Because of the challenges in metering, the steam and natural gas data generally has less resolution and less accurate granular interval data in 15-minute or hourly time frame.



(a)



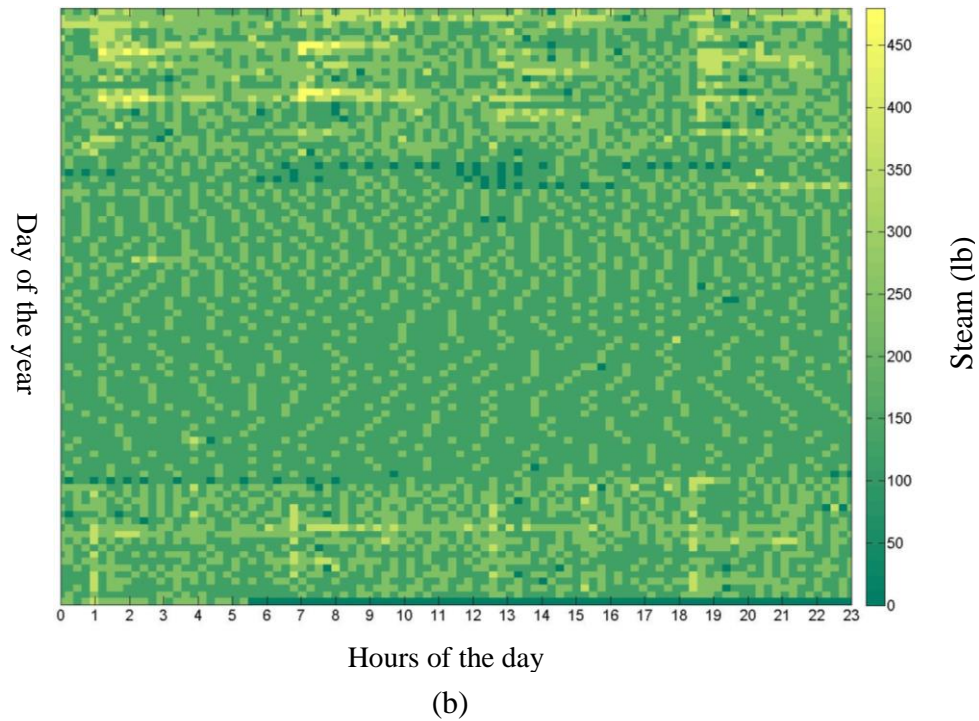


Figure 8: (a) The electricity heat map and (b) the steam heat map for Mitchel Building at UMD campus in 2014

As an example, in the Figure 8, you can find the electricity and steam heat maps for Mitchell Building located at the campus of University of Maryland. This building, which this thesis gets into details more extensively, uses DX system (Direct Expansion) for cooling, and campus steam as the district heating. The electricity heat map shows the daily hours of operation, weekends, spring and winter breaks and the time of the peak cooling loads for this building. However, the steam heat map does not give us as much as details as the electricity heat map for the heating.

#### 4.1.3 Calibration of the Energy Model

Many approximations and estimations are used in the reduced-order energy models that can reduce the model accuracy. One major resource that explicitly provides the calibration method of energy simulations is ASHRAE Guideline 14. This

guideline provides recommendations and statistical analysis to meet sufficient accuracy level in building energy modeling. It provides two indices to represent how well a mathematical model describes the variability in measured data. One index is the CVRMSE and the other is NMBE.

$$\text{CVRMSE} = 100 \times [\Sigma(y_i - \hat{y})^2 / (n - p)]^{1/2} / \bar{y} \quad (8)$$

$$\text{NMBE} = 100 * |\Sigma(y_i - \hat{y}_i)| / [(n - 1) \times \bar{y}] \quad (9)$$

$y_i, \bar{y}, n,$  and  $\hat{y}_i$  are metered building energy data, arithmetic mean of the metered building energy data, number of observations, and simulated building energy data, respectively. For Monthly calibration, it is required by the ASHRAE Guideline 14 to  $\text{CVRMSE} < 15\%$  and  $\text{NMBE} < 5\%$ , and for the hourly calibration, requirements are  $\text{CVRMSE} < 30\%$  and  $\text{NMBE} < 10\%$ .

During the calibration process, sensitivity analysis can help to determine the main parameters. The modeler needs to revisit the model inputs. The definition and schedule for thermal loads are usually the main parameters to modify in the calibration process. After reaching to the required accuracy level mentioned in the guideline, we can express that our model represent the reality of the building. One main barrier to reach to the acceptable accuracy is the quality of the metered data. This topic will be discussed in the following chapters.

## Section 4.2: OpenFOAM CFD Background and Methods

The governing equations as implemented by OpenFOAM are shown below:

Continuity:

$$\frac{\partial \rho}{\partial t} + \nabla \cdot (\rho \vec{v}) = S_m \quad (10)$$

This is the equation derived by conservation of mass for a fluid, where the  $S_m$  term is considered to be a source of mass injection. In urban scale modeling, the steady solution is of concern, and the fluid is assumed to be incompressible due to low speeds and pressures. Also there is no mass injection in the problem. Switching to Einstein summation notation, continuity is reduced to:

$$\frac{\partial u_i}{\partial x_i} = 0 \quad (11)$$

And Momentum (in Reynolds Averaged Form):

$$\frac{\partial}{\partial t} (\rho u_i) + \frac{\partial}{\partial x_j} (\rho u_i u_j) = -\frac{\partial p}{\partial x_i} + \frac{\partial}{\partial x_j} \left[ \mu \left( \frac{\partial u_i}{\partial x_j} + \frac{\partial u_j}{\partial x_i} - \frac{2}{3} \delta_{ij} \frac{\partial u_l}{\partial x_l} \right) - \rho \overline{u'_i u'_j} \right] \quad (12)$$

This equation is derived from conservation of momentum. To incorporate the random three dimensional fluctuations of turbulence, the equation was time averaged to find the mean values for velocities. The very last term is the Reynolds Stress term which contains the fluctuating velocities.

Although the fluid is considered to be incompressible, meaning constant density, there can be small density variations in the flow field due to temperature gradients. While these pressure variances may not be large enough to necessitate compressible flow behavior, they can act as a body force. The Boussinesq approximation for buoyancy allows the momentum equation to account for this

buoyant effect while still allowing the simplification of constant density. OpenFOAM [48] defines the Boussinesq Approximation as valid when:

$$\frac{\beta(T-T_{ref})}{rho_{ref}} \ll 1 \quad (13)$$

$\beta$  is defined as the thermal expansion coefficient, and  $rho_{ref}$  is the reference density of the fluid. The Boussinesq approximation adds a body force term to the momentum equation, which simulates the buoyant flow [49]. The full momentum equation is shown below, modified to account for steady flow, small density perturbations, and a buoyant force. This is the equation used by the buoyantBoussinsqSimpleFoam solver in OpenFOAM.

$$\frac{\partial}{\partial x_j} (u_i u_j) = -\frac{1}{\rho} \frac{\partial p_{rgh}}{\partial x_i} + \frac{\partial}{\partial x_j} \left[ \nu \left( \frac{\partial u_i}{\partial x_j} + \frac{\partial u_j}{\partial x_i} \right) - \overline{u'_i u'_j} \right] - \rho_o g_i \beta (T - T_{ref}) \quad (14)$$

OpenFOAM uses  $p_{rgh}$  in the momentum equation, which is formulated by:

$$p_{rgh} = p - \rho g z \quad (15)$$

Where  $z$  is the vertical position of the fluid element in the direction of the gravity field. This simplifies the pressure field by removing the hydrostatic component.

Temperature is similar to momentum, behaving as a mixture of advection and diffusion. The time averaged energy equation is shown.

Energy Equation (Reynolds Average Form):

$$u_j \frac{\partial T}{\partial x_j} = \frac{\partial}{\partial x_j} \left( \alpha \frac{\partial T}{\partial x_j} - \rho c \overline{v' T'} \right) \quad (16)$$

$\alpha$  is the temperature diffusivity coefficient, calculated using the thermal conductivity, specific heat capacity, and density. The above equations consist of a convective and diffusive part, similar to the momentum equation.

The random fluctuations in turbulent flow represented by the time averaged terms can act as a sort of mixing, or an enhanced diffusivity. A detailed explanation can be found in [50]. Essentially, this enhanced diffusivity can be written as an extra viscous term, so the Reynolds Stress is replaced by:

$$-\overline{u'_i u'_j} = \nu_t \frac{\partial u}{\partial x_i} \quad (17)$$

Where  $\nu_t$  represents the viscosity (diffusion) caused by turbulent fluctuations. In OpenFOAM, a turbulent thermal diffusion term  $\alpha_t$  exists as well, which represents the enhanced mixing of temperature in the flow field.  $\alpha_t$  is calculated by the following equation:

$$\alpha_t = \frac{\nu_t}{Pr_t} \quad (18)$$

The turbulent Prandtl number,  $Pr_t$  is simply defined as the ratio between turbulent viscosity and turbulent thermal diffusivity. While  $Pr_t$  is shown to vary between 0.7 and 0.9, it is often approximated as a constant 0.85 [50]. Often CFD software packages assume  $\nu_t \gg \nu$ , so the laminar viscosity term is neglected. OpenFOAM takes the sum of  $\nu_t$  and  $\nu$ , resulting in an effective total viscosity. The same approach is repeated for thermal diffusivity.

The turbulent viscosity varies throughout the flow field, and must be modeled. For this study, both the realizable k- $\epsilon$  model and the RNG k- $\epsilon$  turbulence models are chosen due to prior success, relative maturity, and ease of implementation [22]. Chapter 5 includes a comparison of the two models which aided in the decision.

The models are based on the theories of turbulent kinetic energy  $k$ , and turbulent dissipation  $\varepsilon$ . Turbulent kinetic energy represents the intensity of the turbulent fluctuations in the flow field, and is produced in regions of high velocity gradient. Turbulent dissipation represents turbulence that is “destroyed”. Turbulence is constructed of many swirling “eddy” flows, which become smaller and smaller as time passes. As the eddies shrink, their kinetic energy is reduced, and eventually becomes negligible. The rate of this occurrence is represented by  $\varepsilon$ . OpenFOAM solves transport equations for  $k$  and  $\varepsilon$  which are as follows:

$$\frac{\partial}{\partial t}(\rho k) + \frac{\partial}{\partial x_i}(\rho k u_i) = \frac{\partial}{\partial x_j} \left[ \left( \mu + \frac{\mu_t}{\sigma_k} \right) \frac{\partial k}{\partial x_j} \right] + G_k + G_b - \rho \varepsilon - Y_M + S_k \quad (19)$$

$$\frac{\partial}{\partial t}(\rho \varepsilon) + \frac{\partial}{\partial x_i}(\rho \varepsilon u_i) = \frac{\partial}{\partial x_j} \left[ \left( \mu + \frac{\mu_t}{\sigma_\varepsilon} \right) \frac{\partial \varepsilon}{\partial x_j} \right] + C_{1\varepsilon} \frac{\varepsilon}{k} (G_k + C_{3\varepsilon} G_b) - C_{2\varepsilon} \rho \frac{\varepsilon^2}{k} + S_\varepsilon \quad (20)$$

The RNG  $k$ - $\varepsilon$  and Realizable  $k$ - $\varepsilon$  model make slight variations to these equations. Once  $k$  and  $\varepsilon$  are found, the turbulent viscosity is calculated via the following equation:

$$\nu_t = C_\mu \frac{k^2}{\varepsilon} \quad (21)$$

The assumptions/approximations used in these equations include: Constant properties, incompressible, low speed, and ideal gas. The  $k$ - $\varepsilon$  assumes fully developed turbulent flow, and while the wind is a highly turbulent phenomenon, there are some questions as to whether the low speed separated regions can be defined as such.

#### 4.2.1 Case Setup

Unlike most CFD software packages, OpenFOAM has no graphics user interface for preprocessing or running jobs. Users must create each cases file tree manually. This section briefly overviews the setup of OpenFOAM cases to aid in understanding of the program.

Each OpenFOAM case folder contains three sections: constant, system, and the time folders [51]. Constant contains the simulation geometry and the mesh information, as well as relevant transport properties and turbulence modeling options. System folder contains controls for certain simulation parameters, such as time step and number of iterations. In addition, discretization schemes and residual controls can be modified here as well. In the time folders, all of the variable values are stored for the corresponding time step. The first time folder (0) contains the initial conditions for the simulation (or initial guess for steady simulations). It is common practice to specify the boundary conditions in this folder, although they can be modified in later time steps.

Simulations in subsequent chapters make use of the GAMG (Geometric-algebraic multi-grid) solver for pressure. This solver is selected due to good performance on large domains of many cells [52]. The solver speeds up simulations by initially solving the pressure equation on a very coarse grid, and iteratively solving while increasing the number of cells, providing initialization from the previous coarser solution. For all other variables, the smooth solver is used, which tended to improve simulation convergence time.

As Virtual PULSE is used for the energy modeling section, the building footprints are all drawn. Then, based on the height of the buildings and the building footprints, it generates a STL file of the buildings, and a ST file of the ground. The ground.stl file is in the size of the domain that is described in the next sub-section.

#### 4.2.2 Domain

The domain for urban simulations implemented OpenFOAM follows recommendations suggested by previous public guidelines and urban thermal environment studies [53] [54]. Figure 9 presents an example CFD domain for flow over a building.

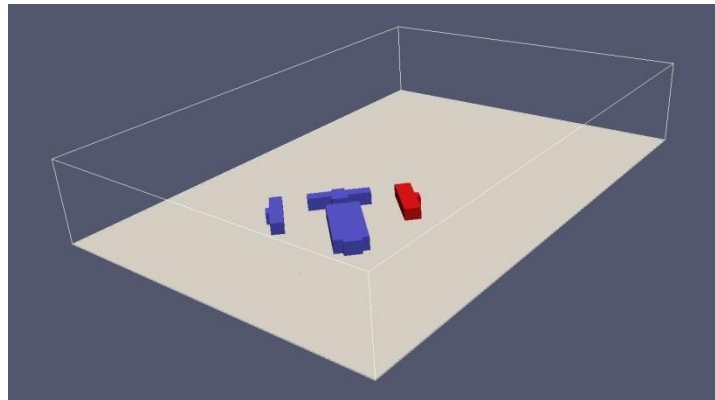


Figure 9: Example of CFD domain for flow over a building neighborhood

The building in red in the Figure 9 represents the building of the primary focus, calling that building “primary” and the other buildings “secondary”. The primary building(s) will have higher mesh resolution and the results from CFD will be more accurate, while secondary buildings represent surface roughness for the airflow seen from the primary building view.



For a building neighborhood with maximum height  $H$ , the domain is set to a height of  $10H$ . The sides of the building are a minimum of  $5H$  from the sides of the domain. The domain inlet is placed  $5H$  from the windward edge of the front building, and the outlet is  $15H$  from the leeward edge of the last building, to allow for a fully formed wake.

Regarding boundary conditions, for all variables, the top and sides are treated as slip conditions. For scalars, this is equivalent to a zeroGradient condition, indicating that far from the building, the fields are uniform and undisturbed. For velocity (a vector) the normal component is zero (no outflow on the top and sides) and the tangential component is zeroGradient (keeps the flow uniform).

At the inlet, all variables except velocity and temperature are set to zeroGradient. Temperature and Velocity are special cases, with either specified values or profiles, which will be discussed later in this section. The outlet sets all variables to zeroGradient, except pressure. Here pressure is set to a reference of 0. This allows all pressures in the domain to be referenced to the value of 0, which can be convenient for quantifying pressure drops.

Appropriate wall functions are specified for the ground and building surfaces, discussed later in this chapter.

#### 4.2.3 Meshing

The CFD simulations in this thesis use unstructured meshes generated by SnappyHexMesh for the computational grid. SnappyHexMesh uses an innovative cell splitting method to essentially merge a background mesh with a STereoLithography

(STL) file. The result is capable meshing software which nearly automates the process of meshing.

Before SnappyHexMesh can generate the mesh, both a background mesh and a geometry file are required. The background mesh can be created with OpenFOAM's built in blockMesh tool. The background mesh is essentially the fluid domain, so blockMesh should be used to choose the domain size, as well as the inlet, outlet and ground patches. Note that best results from meshing occur when the background mesh cells are near square. Also, the cells must be small enough to intersect with the STL geometry at least once.

Once the background mesh is obtained, and the STL file is created, it must be ensured that the STL file coordinates are aligned correctly with the background mesh. SnappyHexMesh then uses three steps to create the mesh. The first step, the castellated mesh, SnappyHexMesh finds the intersection between the STL file and the background mesh. From here, the cells at the intersection are split in each direction, dividing the cell into eighths. The cells are split again, depending on how many divisions the user specified. The group of cells surrounding the intersection cells are split as well, but one division less than the group closest to the geometry. Farther back from the geometry, these groups of cells are divided as well, but one division less yet. This process continues until sufficiently far away from the geometry that the cells are the original size of those created in the background mesh. At this point, the cells contained inside the geometry are removed, and the cells at the intersection are the new wall boundary. Figure 10 illustrates the castellated mesh step in SnappyHexMesh.

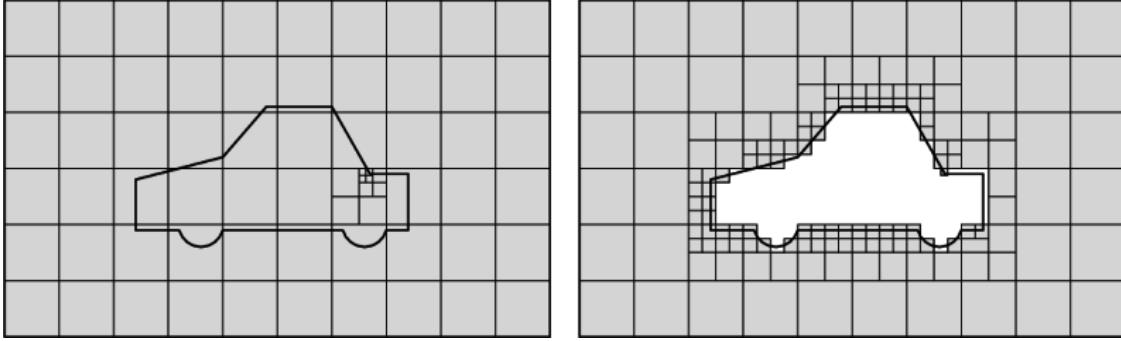


Figure 10: SnappyHexMesh cell snap procedure [51]

The second step is the surface snap. The mesh created in step one is completely defined by cubic cells. If the geometry represented is completely rectangular, then the mesh can approximate its shape very closely. Otherwise, any angles will be represented by jagged cell edges. The snap step will translate and cut the intersection cells to attempt to approximate the geometry shape. In a case where all of the geometry has been simplified to rectangles, the snap step is not necessary. An optional “addLayers” step can add thin layers of cells against the boundary, which can help resolve the thin boundary layer without increasing the global cell count significantly.

SnappyHexMesh will assign a boundary condition label based on the solid name inside the STL file. If an STL file has multiple solid labels, then each one will be imported by SnappyHexMesh as a separate boundary patch. This can be useful if different boundary conditions are required for different sections of geometry. Different walls of a building may have different temperatures applied, for example.

One main parameter that is described in the literature review chapter was  $y^+$ .  $Y^+$  is the non-dimensional distance between the wall surfaces to the first adjacent cell to the wall. In order to resolve the boundary layer flow using the

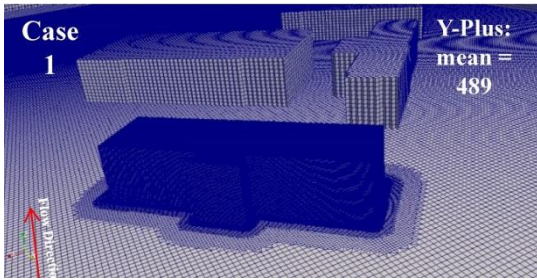
standard wall functions,  $y^+$  needs to be under 300, preferably under 100. One of the findings of this thesis is the two main parameters that affect  $y^+$ . The first one is the level of refining the mesh around the object which in my case is the primary building. There is a trade-off between level of refinement and the number of cells. While the number of cells increases,  $y^+$  value improves, however meshing and solving the airflow takes much longer. Therefore, the intent in this thesis was to find the optimum level of refinement. In the modeling the airflow in the scale of neighborhood, the typical number of cells in the domain is between 3 to 10 million. Using processors in parallel both in meshing and solving the domain is quite lower the computation time drastically.

The other main effective parameter in the value of  $y^+$  is the type of mesh refinement. In OpenFOAM, users are able to create the most refined mesh (the space with the fine mesh) by a distance from the surface of the object, or by a box. It is shown in Figure 11 that the box type of fine mesh with the sufficient level of refinement results in the acceptable range of  $y^+$  throughout the surface of the primary building. The boxes in the Figure 11 show the second and third quartiles of the data and show the median of the data with a horizontal red line inside the box. Each level for refinement results in cutting the cells in half in each direction, making the number of the affected cells 8 times of the initial cells. In the Mitchell neighborhood, the acceptable range of  $y^+$  was reached with box method and 7 level of refinement in the refinement box around Mitchell building. Other buildings had lower levels of refinement; hence higher  $y^+$  value is resulted. Results showed that the effect of box or

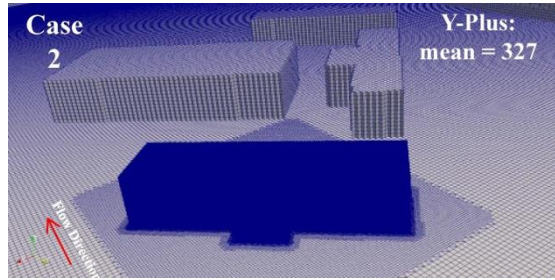
distance mesh is seen mainly in the cases that the wind blows diagonally relative to the buildings. In the other cases, the two method of meshing are similar in the results.



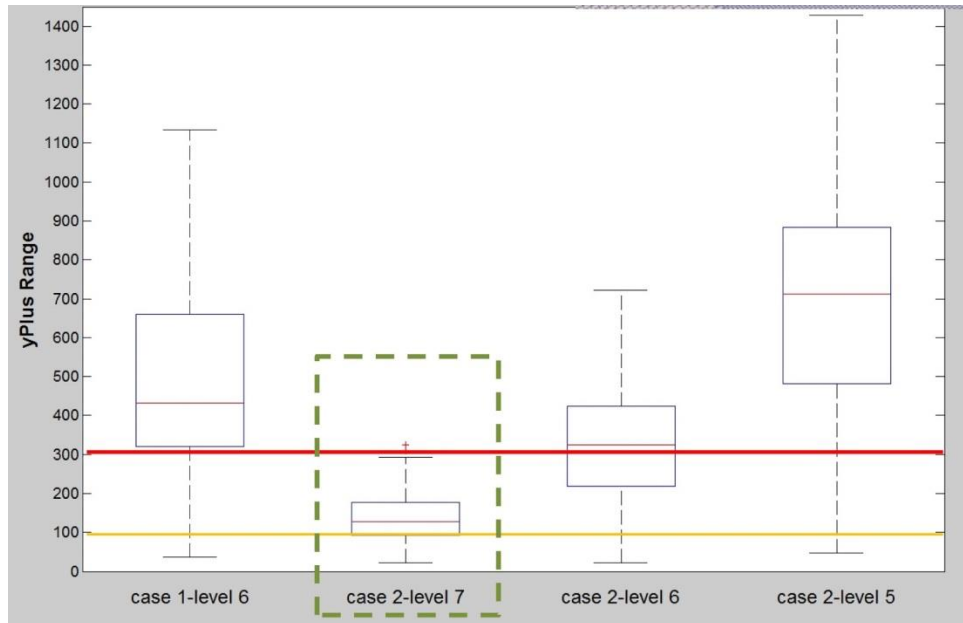
(a)



(b)



(c)



(d)

Figure 11: (a) Mitchell building and the surrounding neighborhood (b) the distance method mesh refinement (c) the box method mesh refinement (d) the  $y^+$  value comparison on surface patches

#### 4.2.4 Wall Functions

The turbulence models chosen for the study facilitate standard wall functions as boundary conditions. While standard wall functions may reduce accuracy for certain flow conditions, they greatly reduce computational time. The studies in this thesis make use of standard smooth wall functions across building surfaces. On the ground surface, atmospheric wall functions are used to approximate the  $v_t$  and velocity profiles occurring in urban atmospheric boundary layers.

#### Section 4.3: Method of Combining CFD and Energy Simulations

In this thesis, footprints of the buildings in a neighborhood are drawn using standard shapes in Virtual PULSE. The simplified geometry of the buildings is created based on the number of floors, floor to floor height, and window to wall ratio. An STL file of the neighborhood is used in modeling the outdoor airflow in a CFD domain. The method of case setup, domain size, and meshing is described in the prior section. To validate the CFD case, the Radiance simulation results are used as constant heat flux for the boundary conditions on the building surfaces and the ground. A solver suitable for steady, incompressible, and turbulent flow with buoyancy effect approximations (buoyantBoussinesqSimpleFoam) is used to resolve neighborhood thermal boundary layer flow.

To investigate the wind effects in Chapter 6, an iso-thermal CFD case is used. The iso-thermal CFD solution indicates the wind velocity around the primary building in different directions affected by the other buildings in the neighborhood. By measuring the wind velocity in eight main directions, wind multipliers for each

direction are created. Then the wind velocity column in weather data file, which is an input to the energy model, is modified by the wind multipliers. The modified weather data is used in EnergyPlus to see the effects of wind direction and velocity in the energy model.

EnergyPlus is used to calculate the surface temperatures of buildings in urban neighborhoods independently of the CFD simulation. While there are examples of studies which use CFD to calculate the CHTC for EnergyPlus, the accuracy of CHTCs from CFD can be highly questionable. CHTC's are highly dependent on near wall modeling, so using standard wall functions does not provide high enough resolution to accurately calculate the CHTC. The CHTC correlations in EnergyPlus are the result of significant research [55]. Using these correlations allows EnergyPlus to run a full year energy study for a building very quickly.

In summary, the goal in combining the energy model and the outdoor airflow model is to refine the energy model assumptions in considering outdoor weather parameters, especially wind. While wind velocity is direction-dependent, EnergyPlus assumes a constant wind velocity at all the facades. However, the presence of other buildings can make this assumption untrue. Measuring wind speed blowing from different directions, close to the building leads us to a modified weather data. Then the weather data improves the energy model accuracy.

## Chapter 5: Framework Validation of CFD Results for an Actual Case Study

This chapter is concerned with using OpenFOAM CFD to model actual urban areas in order to validate the use of OpenFOAM for use in predicting local temperatures in urban areas. OpenFOAM is gaining popularity as a simulation tool for studying urban environments. Researchers are beginning to publish papers using the tool for urban prediction of pollutant dispersion [56] [57], and urban microclimate study [58]. Nevertheless, the implementation of OpenFOAM and EnergyPlus in this thesis is for the most part unique. More validation can strengthen the results. This chapter focuses on a case study of real buildings at the University of Maryland campus. The goal of the study is to validate local temperature results found from OpenFOAM with measured data obtained in the actual urban environment. In summary, air temperature is a proxy to validate the airflow model.

### Section 5.1: Background

A neighborhood on the east side of the campus of the University of Maryland was selected. This campus neighborhood consists of four buildings of Mitchell, Administration, Lee and Reckord Armory. Reckord Armory is a recreation building type, while the other buildings are office type buildings. The target building, or as I call in the CFD setup, primary, is Mitchel Building. The reason that this building is chosen is that the surrounding of that building is very suitable for installing



temperature sensors with so many various poles, shaded and unshaded. Figure 12 shows the satellite and bird's eye view for this campus neighborhood.

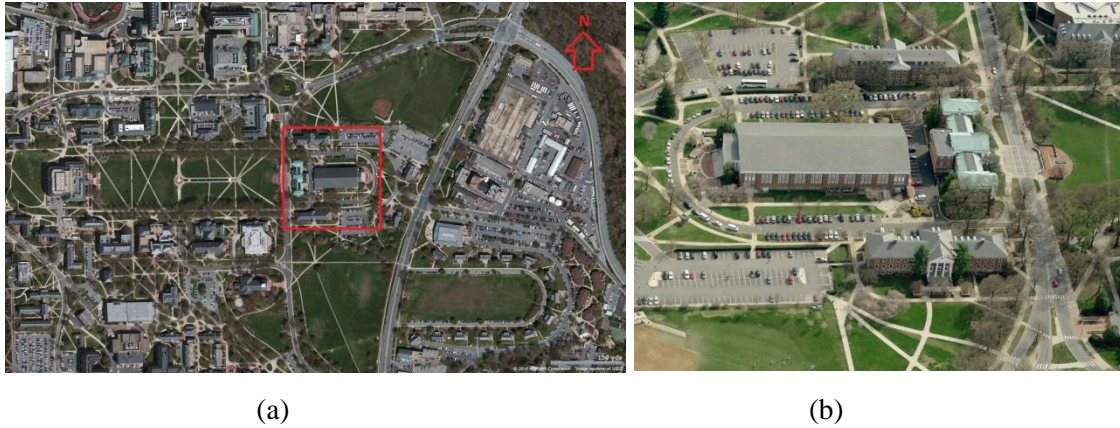


Figure 12: (a) Satellite view and (b) Bird's eye view of the Mitchel building and the surrounding neighborhood at the University of Maryland

The figure shows the relative size of the buildings as well as the environment near them. There is a semi-dense urban environment directly southwest and northwest of the neighborhood.

## Section 5.2: Data Measurement Procedure

### 5.2.1 Instrumentation

The temperature was collected during June 23<sup>rd</sup> to June 27<sup>th</sup> 2014 around Mitchel building. The outdoor air temperature measurements were taken using iButton sensors. iButton sensors are a kind of digital thermometer. The figure shows that the iButton sensor is slightly smaller in diameter to a quarter. The iButton sensor is convenient due to the small size and wireless connectivity. While conventional thermocouples offer faster response time and higher accuracy, the expense and

difficulty of using wired sensors necessitated the use of the iButton [11]. The reported accuracy of the sensor is  $\pm 0.5^{\circ}\text{C}$  from  $-10^{\circ}\text{C}$  to  $+65^{\circ}\text{C}$ , and the precision is 0.0625. Aluminum foil was used to shield the sensor from direct solar radiation.



Figure 13: Preparing iButton sensors for the temperature measurements, avoiding direct sunlight and rain using some aluminum foil

### 5.2.2 On-Site Data Collection Setup

The temperature data was collected at eight locations around Mitchell building shown in Figure 14. Mainly light poles and other existing poles were used for installation. The measurement was done at 1m, 1.5m, and 2m height at each location. Moreover, numerous Infra-Red (IR) photos of the building and ground surfaces were taken using FLIR E-40 IR camera. The IR photos were taken in two-hour intervals from 9 am to 5 pm on two days during the experiment.



Figure 14: The location of the iButton temperature sensors in the experiment in July 2014 around Mitchell building on the University of Maryland campus

A sample of the IR photos is presented in the following sections along with the CFD case results. The CFD study will focus on these locations to determine the accuracy of CFD simulations using OpenFOAM. Before starting to create CFD model, we need to know about the wind velocity and direction at the time of the experiment. Using the Actual Meteorological Year (AMY) data from College Park airport weather station (KCGS) for 2014, a wind rose was created. The AMY data consists of all the

weather parameters for all the hours of a specific year. The wind rose in the Figure 15 is for College Park (UMD) during the experiment

The wind rose indicates that the prevailing wind is from southeast during the experiment. Knowing the wind direction is necessary for setting up the CFD domain. As the wind is from southeast, the neighborhood is rotated 45 degrees clockwise relative to +y axis, which is assumed to be the wind direction in the CFD domain.

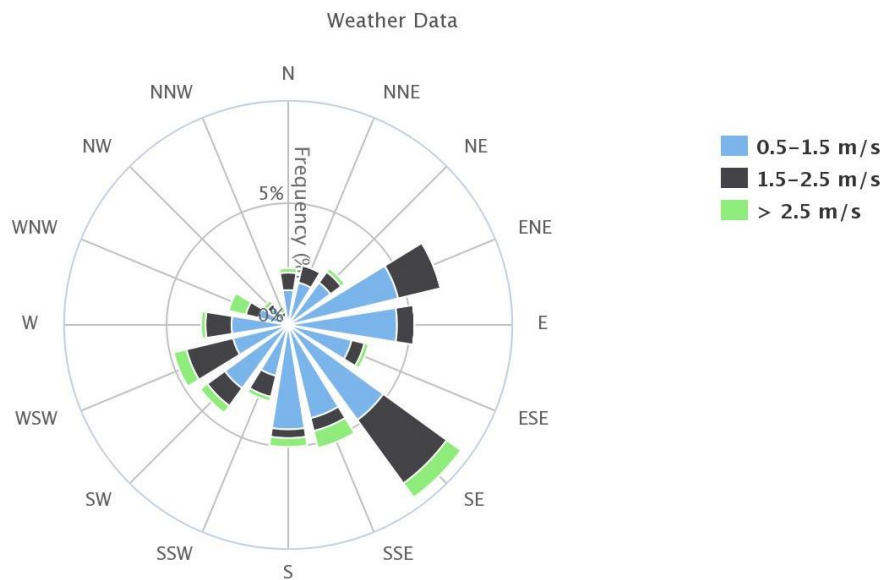


Figure 15: Wind rose for College Park, MD, during the experiment on June 23<sup>rd</sup> to 27<sup>th</sup>, 2014 using AMY data for the data-source and highcharts.com for visualization

### Section 5.3: Site-Specific CFD Case

The CFD case was setup based on a specific time and date that relatively high air temperature occurred. June 24<sup>th</sup> 2014 at 1 pm was chosen as the date for the CFD model and then the comparison and validation. Based on the AMY data for College Park, MD at the selected time, the air temperature was 28.2°C (82.8°F)



### 5.3.1 CFD Case Inputs

The buildings and the ground are imported into OpenFOAM using STL format. A background mesh is created using the OpenFOAM built-in tool named blockMesh. The background mesh is in the size of  $20\text{m} \times 20\text{m} \times 20\text{m}$  cells creating a giant domain of  $420\text{m} \times 600\text{m} \times 100\text{m}$ . As the domain is so big, the way the fine mesh is made is so important. Refining the mesh is done by snappyHexMesh. There are boxes of refined mesh created, one rough refined box close to the ground up to 30 m height, one finer refinement box around the neighborhood, and one very fine box of mesh around the primary building. You can see the details in the Figure 16.

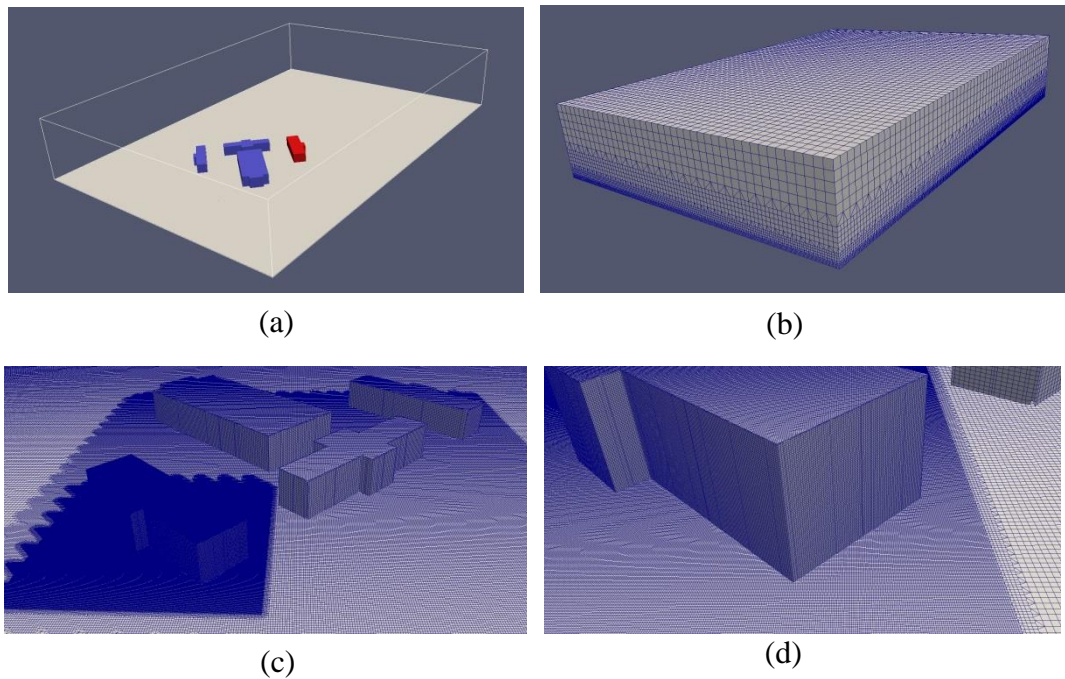


Figure 16: (a) Mitchell building, primary, and the surrounding neighborhood, secondary buildings, STL geometry (b) the final mesh domain and the refined mesh close to the ground (c) secondary and primary buildings refined mesh (d) fine mesh on the primary building

The thermal boundary conditions for buildings are applied as described in Chapter 4. Here we review them in summary. At the inlet, all the variables except temperature and velocity are set to zeroGradient. Temperature is fixed at 28.2°C (82.8°F) at the inlet. The inlet velocity is defined based on a profile using the following equation, implemented in OpenFOAM as the atmBoundaryLayerInletVelocity boundary condition [59]:

$$U = \frac{U^*}{\kappa} \ln \frac{z - z_g + z_0}{z_0} \quad (22)$$

Where  $U^*$  is the friction velocity,  $z$  is the elevation above the ground,  $z_g$  is the elevation of the ground, and  $z_0$  is the roughness length of the ground.  $z_0$  was defined as 0.3m in this case, due to the mostly small obstacles preceding the buildings of interest. The maximum of the inlet velocity is 5m/s.

The outlet sets all variables to zeroGradient except pressure. Pressure is set to a reference of zero. The top and sides have the slip condition which equals zeroGradient for scalars. The building and ground surfaces have the constant heat flux condition. The value of the heat flux is imported from Radiance solar radiation simulation and assigned to each patch for the time of the experiment 6/24/2014 at 1 pm. The heat fluxes are the result of the short-wave analysis of solar radiation within the neighborhood. Figure 17 shows the high intensity of the solar radiation at the time of the experiment.

Two turbulence methods, Realizable k- $\epsilon$  and RNG k- $\epsilon$  are tested to be used in the comparison. The details of the files in the system folder, including the relaxation factors and convergence criteria in fvSolution file are placed in thesis appendices.

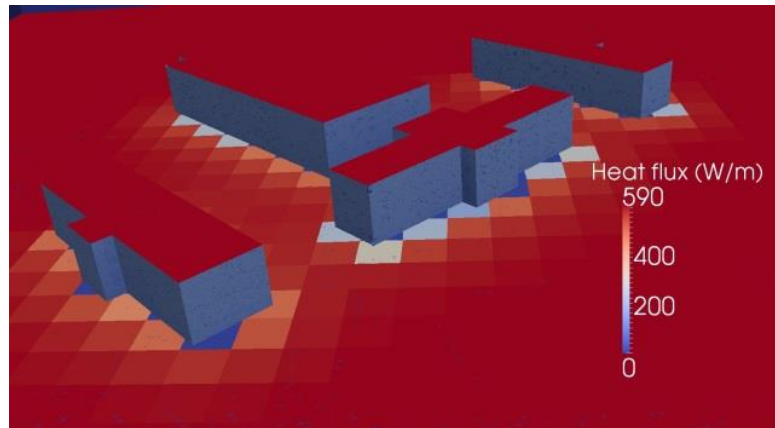


Figure 17: The constant heat flux resulted from Radiance solar radiation simulation

### 5.3.2 CFD Simulation Results

The CFD case resulted in more than 15 million cells and took more than 7500 iterations to converge. This case has a  $y^+$  mean of 550 and maximum of 1200 on specific spots. Figure 18 illustrates a sample output which is the surface temperature in Kelvin.

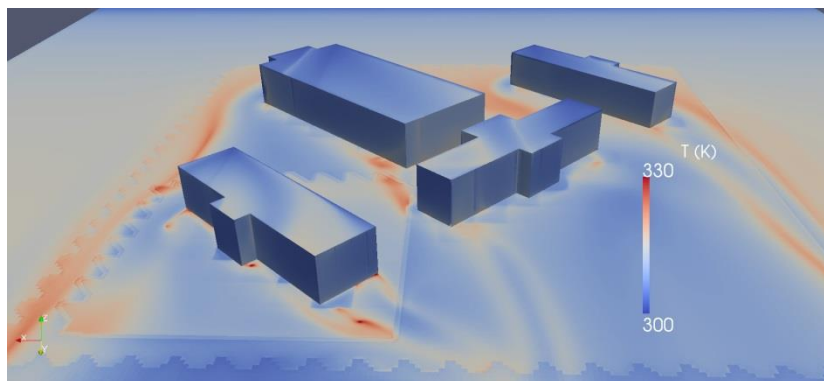


Figure 18: CFD results, the surface temperature at the time of the experiment 6/24/2014, 1 pm

### Section 5.4: CFD Simulation and Collected Data Comparison

We have collected on-site air temperature from a campus neighborhood and modeled the airflow in a CFD case for 6/24/2014 at 1 pm. Actually, temperature here

acts a proxy to show how accurate a CFD model can be. The temperature measurements were done at eight locations. However, three of the locations had issues in gathering the data. Hence, the comparison is done in the table below at five locations at three heights of 1m, 1.5m, and 2m.

Table 1: Temperature data from two CFD turbulent simulations compared to measurement

Location A (°C)	Realizable k-ε	RNG k-ε	iButton ±0.5°C
1 m	31.1	30.4	30.5
1.5 m	30.8	30.2	30.6
2 m	30.6	30.2	30.5
Location B (°C)			
1 m	30.2	30.0	30.6
1.5 m	29.5	29.2	29.7
2 m	29.3	29.1	29.8
Location E (°C)			
1 m	30.7	30.5	30.3
1.5 m	30.0	29.9	30.2
2 m	29.9	29.4	30.5
Location F (°C)			
1 m	30.4	30.4	29.4
1.5 m	29.8	29.8	29.4
2 m	29.6	29.6	29.3
Location G (°C)			
1 m	31.1	30.4	30.4
1.5 m	30.9	30.3	30.2
2 m	30.8	30.3	30.4

From Table 1, it is clear that RNG k-ε is closer to the measurements. The CVRMSE for the Realizable k-ε is 6% relative to the measurements, while this parameter is 2% for the RNG k-ε. This is consistent with another recent study with the same scope of work [22].



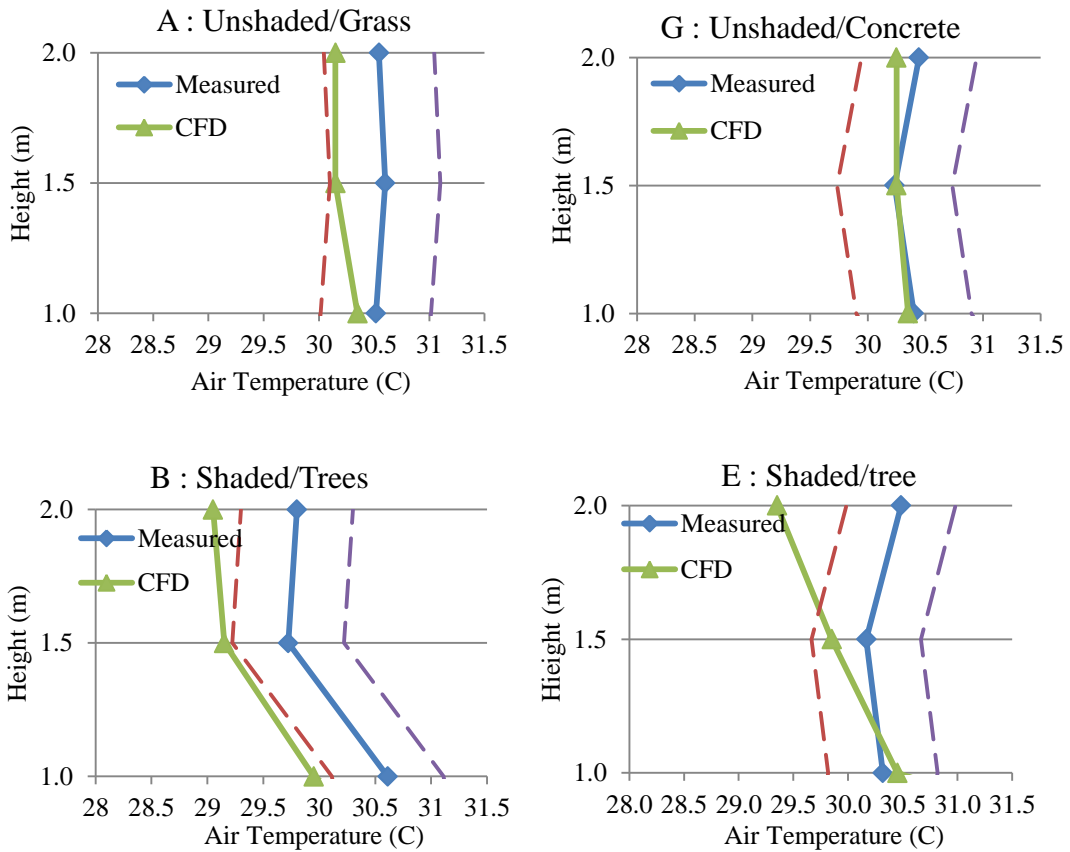


Figure 19: The measured and CFD model results at four locations. Dash-lines represent iButtons minimum accuracy range

In

Figure 19, the values from the Table 1 for RNG k-ε CFD model and measured data are illustrated at four locations. The dash-lines represent the iButton temperature sensors minimum accuracy of  $\pm 0.5^{\circ}\text{C}$ . In general, the value of the CVRMSE and the figure above show that the model is sufficiently accurate in representing the temperature field in the neighborhood. However, we can see that it is most accurate in the unshaded areas, while it can be far from reality to some extent in unshaded spots. The main reason is that this CFD model does not include trees and other greeneries in

the model. Thus, the simplification that I made in including trees and greeneries can lead to some errors in the shaded areas. Moreover, for solar radiation analysis in Radiance, it is assumed that all the ground patches or surfaces are concrete. We can see the result of this assumption below in Figure 20. The Figure 20 shows the IR photos of the primary building surfaces and also ground along with the CFD results. The comparison shows that the model is fairly accurate on the unshaded areas and it is less accurate on the shaded areas. One other source of difference between the

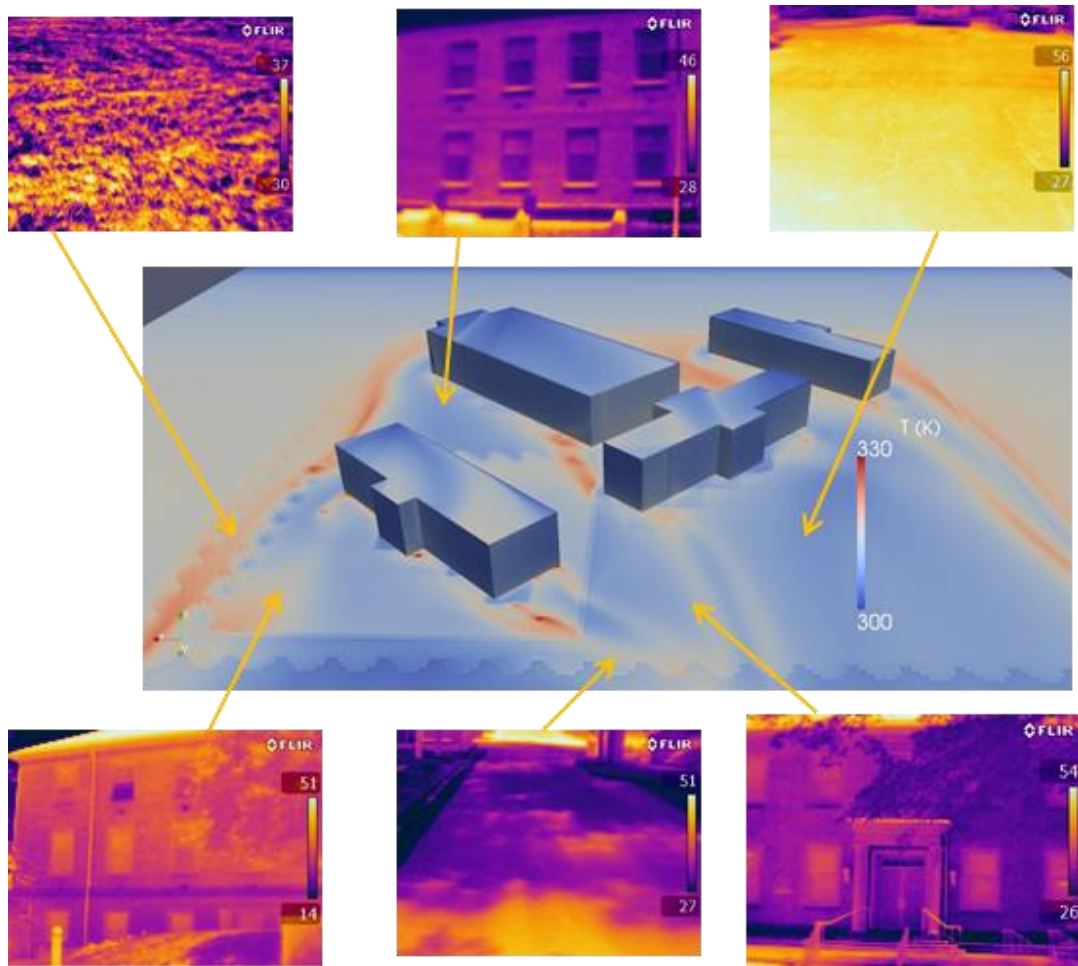


Figure 20: The surface temperature in Kelvin from CFD model along with the IR photos at the time of the experiment

model and the measurement is that as the greeneries such as grass are not modeled in this CFD simulation, the evapotranspiration is not seen. Ignoring this heat transfer mechanism has resulted in less accurate CFD output in the grass or green areas.

The comparison led to this point that the temperature field is generally predicted well by the CFD model at the time of the experiment. As the energy and fluid equations are coupled in nature and in the numerical solution, we can reach to say that the model has represented the urban boundary layer to a good extent by using temperature as the proxy. However, the unshaded and grass areas were less accurate due to excluding trees and grass from the radiation analysis and CFD simulation.

## Chapter 6: Wind-Focused CFD and Energy Studies at an Actual Neighborhood

This chapter builds upon the methodology and findings from the previous chapters in order to design a set of CFD simulations to quantify the effect of wind in building energy use. The gap which led us to go this path was that energy models do not take the neighborhood effects into account. Energy simulation programs such as EnergyPlus include the buildings in the close proximity shading on the target building in solar radiation analysis. However, they do not see the presence of other buildings in considering outdoor temperature and wind. Local temperature in an urban area is mainly dependent on a city-scale which is not in the scope of this thesis. However, wind velocity and direction can greatly be influenced by the buildings around and can be seen as a neighborhood effect. This chapter aims to demonstrate a simplified approach to model this neighborhood effect.

Wind has impacts on the building energy use through two main parameters. One of these parameters is the exterior convective heat transfer coefficients and the other one is infiltration. The wind velocity and direction can both change the flow regimes on the building surfaces and as a result change the convective heat transfer coefficients. However, this is considered being an indirect impact to the building heat gain or heat loss through the walls or roof.

The main impact of wind is on the infiltration. The wind velocity is present in all of the infiltration models discussed in the Literature Review, equations (1) to (3). To be accurate, each building facade can see different wind velocity due to the presence of the other buildings around. This study keeps the assumption that the

facades see the same velocity, however the modification the velocity occurs as the whole building sees.

The main idea is to use CFD models to correct the wind velocity that the building sees in the neighborhood. The following section explains how to setup eight separate CFD cases which represent wind blowing from 8 main directions. By measuring wind at the windward facade in these CFD cases, this study managed to create wind multipliers which are the average wind velocity close to the building relative to the inlet wind velocity.

Wind multipliers are used to modify the wind velocity column in the weather data. This modified weather data is then used to calibrate the energy model. With a calibrated energy model, we can be sure that the model represents the actual building accurately. Then by trying the original weather data and the modified one, we can actually see the effect of wind in the building energy use.

In order to show this process, I have picked the same campus neighborhood at the University of Maryland in the last chapter with Mitchell building as the target. First I show the CFD simulation cases and wind multipliers. Then in the next section, I go through creating a baseline energy model. In the last section, the energy model gets calibrated and then based on the calibrated model; the study will see the effect of the wind multipliers in the energy model.

### *Section 6.1: CFD Simulation and Wind Multipliers*

Here the CFD cases are based on the previous chapter with two main differences. First of all, the focus is to see the wind effects solely. Therefore the

temperature variations through the domain are neglected. This means that the CFD cases in this chapter are all iso-thermal. Running an iso-thermal CFD case with the previous flow conditions, such as steady, incompressible, and turbulent needs another solver. The suitable solver in OpenFOAM for this application is simpleFOAM which is the simplified version of the solver buoyantBoussinesqSimpleFOAM with no buoyancy approximations.

The second difference with the previous CFD cases in this thesis is the assumption that we make for the inlet velocity. To see the wind velocity changes in different directions, we can easily try different direction with a specific speed. However, it is not easy to determine a specific wind speed for a neighborhood throughout a year. Wind speed can vary greatly at a location even in a day. To simplify this complexity, the study assumed an inlet velocity of 1m/s in any direction. This assumption can simplify the details to a great extent. By inlet velocity of 1 m/s, the building might see a wind speed of 0.7 m/s in a specific direction. This does not mean that if in a real condition the prevailing wind speed is 10 m/s, the building sees the wind speed of 7 m/s. However, this aims to be a step forward to take wind speed variations into account in energy models.

It is assumed that wind blows at 1 m/s in eight main directions, including North (N), Northeast (NE), East (E), Southeast (SE), South (S), Southwest (SW), West (W), and Northwest (NW). For each direction there is a CFD case. In these CFD cases, the domain is in the same place and wind blows in +y direction, but the buildings are rotated 45 degrees for each case relative to the previous case. Figure 21 shows the building rotation.

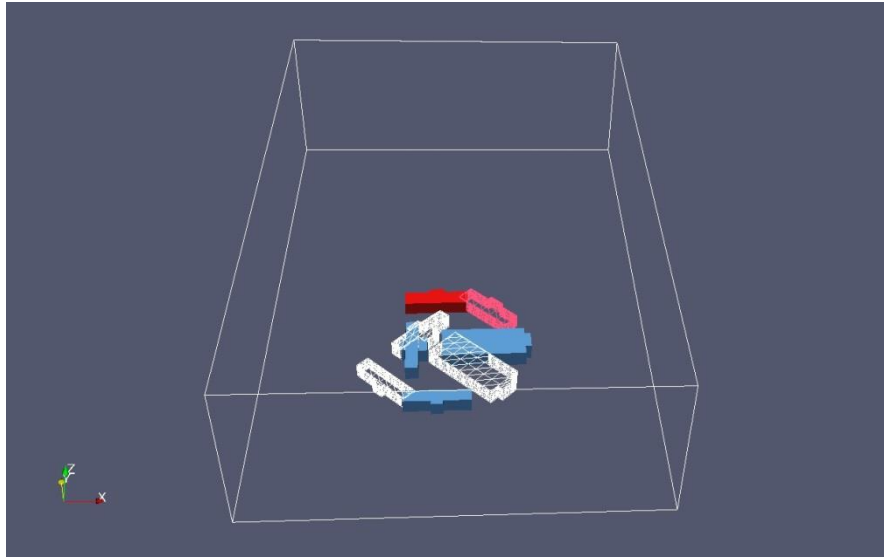


Figure 21: An example of the buildings rotation in creating eight CFD cases

As there is no temperature variation, the CFD cases are less complex and the mesh is less refined. The method of meshing is still the same but the level of refinement is generally lower. The resulted grid is about 6 million cells for all the eight cases.

To take the wind velocity measurement close to the building, it is important to determine where can be the good representative of the wind velocity that the building sees. In addition, we need to make sure that we are not measuring in the boundary layer of the building itself. Thus, it is required to know an approximation of the boundary layer thickness on the target building surface. This study has simplified the building surface as a flat plate experiencing a turbulent flow with the prevailing speed of 1 m/s. Based on the power law expressions, the layer thickness [60] will be:

$$\frac{\delta}{x} = \frac{0.16}{Re_x^{1/7}} \quad (23)$$

where  $\delta$  is the boundary layer thickness at the distance  $x$  from the tip of the plate. Based on this equation, the boundary layer of the building does not exceed 2m.

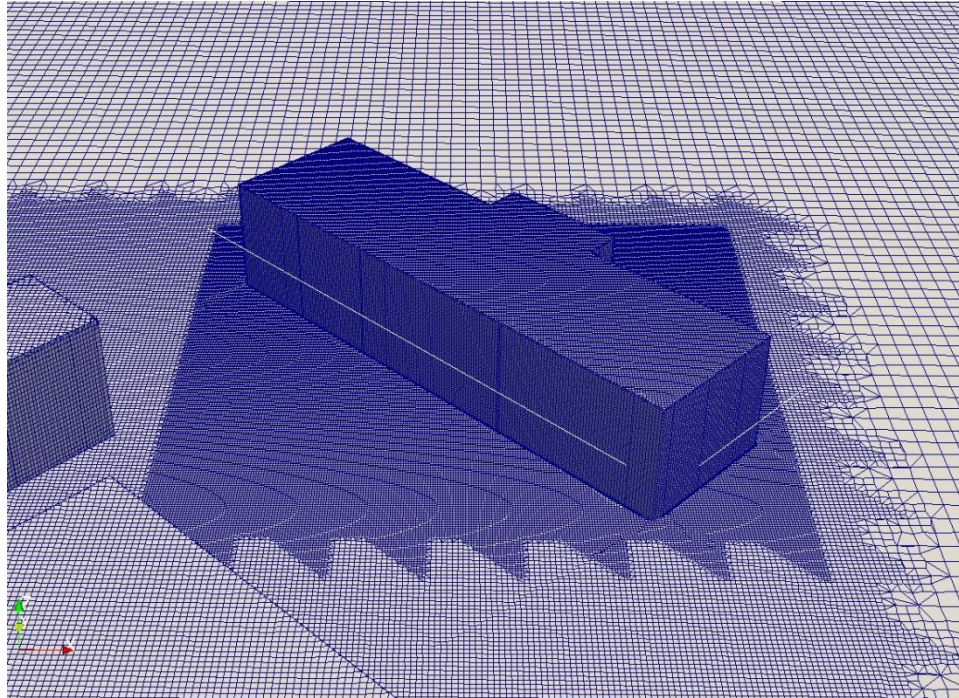


Figure 22: One of the wind velocity measurements at the windward facade on the two white lines

This study has made the measurements in CFD at the 5m distance to be in the safe side making sure that wind speeds are read out of the boundary layer of the target building. The wind speeds measured at the weather stations are usually collected at 10m height from the ground. So the wind velocity in the TMY3 or AMY weather data file represents the wind speeds at that height. Hence, the measurements in the CFD model are done at 10m height from the ground, 5m away from the building facade, as shown in Figure 22.

For the cases as the Figure 22, the windward facade is assumed to be two, as the wind blows with an angle of 45 degrees relative to the windward facades. For the other cases, it is only one windward facade.



After taking the wind velocity, the wind multipliers are generated using the proportions of the average of the measurements and the inlet velocity. As the inlet velocity is 1 m/s, the wind multiplier in each direction is the average value of the measurement at the windward facade(s). The summary of the collected data through CFD cases is shown in the figure below. The red horizontal lines, which are the average of the data in each direction, represent the wind multiplier in that direction.

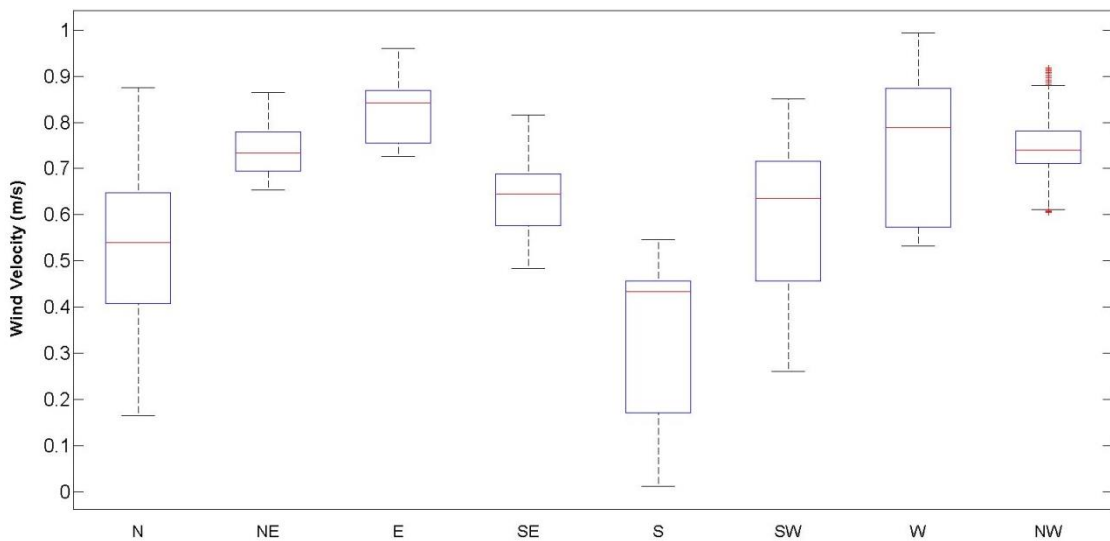


Figure 23: The measured wind velocity at the windward facades in 8 directions for Mitchell building

The measured data shows that the building sees the highest speeds in the east and west directions and sees the lowest speed in the north and south directions. This was completely predictable as the target building, Mitchell, is not surrounded by the east and west by any other building and all the buildings are on the south side of it. The other point is that the wind speeds can vary greatly based on the direction from 0.4 in the south, to 0.8 in the east direction. The wind velocity in the AMY weather data for College Park, MD 2013 and 2014 multiplied by the related wind multiplier in the Table 2. As the wind direction is divided in 8 main directions, there is at most the

error of 22.5 degrees in considering the actual wind direction. A MATLAB code is used in applying the multipliers to the wind velocity column in the AMY weather data file.

Table 2: The wind multipliers and the affected wind direction range

Wind direction	Wind direction range	Wind multiplier
North	-22.5° to 22.5°	0.626
Northeast	22.5° to 67.5°	0.740
East	67.5° to 112.5°	0.738
Southeast	112.5° to 157.5°	0.641
South	157.5° to 202.5°	0.403
Southwest	202.5° to 247.5°	0.589
West	247.5° to 292.5°	0.787
Northwest	292.5° to 337.5	0.746

By having a modified wind velocity, the modified weather data files can be used as inputs in the energy model. The following section elaborates on how to create a baseline energy model. In the last section the baseline energy model gets calibrated with this modified weather data along with other calibration inputs. In the end, the calibrated model will be used in comparing the modified vs. unmodified weather data in the energy model.

Section 6.2: Baseline Energy Model

The baseline energy model is a simplified energy model of the target building with the least details and complexities. Most of the inputs for the baseline are gotten from University of Maryland public data online and the occasional visits to the building. The baseline energy model is created using Virtual PULSE online platform

which sets up an OpenStudio model. The inputs used in the baseline energy model are listed in Table 3. Mitchell building is a medium size office building built in 1958.

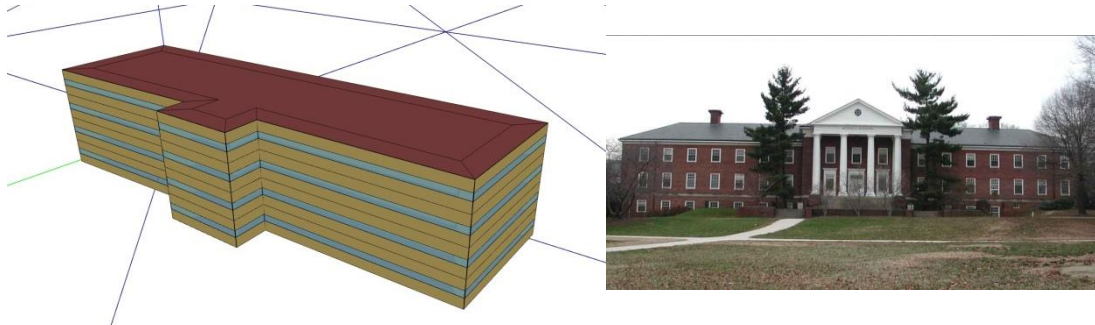


Figure 24: The OpenStudio model of Mitchell building as the baseline energy model

Table 3: The summary of the baseline energy model inputs in Virtual PULSE

Building parameters	Baseline energy model inputs
Geometry and shape	T shape 4 floors Floor to floor height: 3m (10 ft)
Information	Year built: 1958 Type: office Weather: AMY College Park, MD 2014
Construction	DOE Ref Pre-1980
Spaces	Window to wall ratio: 33% Thermal zones : perimeter and core zoning with single space type Perimeter zone depth: 3m (9.8 ft)
Loads	Lighting: 20 W/m <sup>2</sup> Electric equipment: 10 W/m <sup>2</sup> Infiltration: 0.002 m <sup>3</sup> /m <sup>2</sup> s of exterior surface area (0.4 cfm/ft.min)
HVAC	Rooftop VAV with reheat DX for cooling District heating Fan efficiency: 70% Ventilation: 0.06 cfm/ft <sup>2</sup> + 5 cfm/person
Simulation result	Area: 4217 m <sup>2</sup> (45400 ft <sup>2</sup> ) Actual area: 4200 m <sup>2</sup> (45212 ft <sup>2</sup> )  EUI: 1135 MJ/m <sup>2</sup> (100 kBtu/ft <sup>2</sup> ) Actual EUI: 854 MJ/m <sup>2</sup> (75.2 kBtu/ft <sup>2</sup> )

Based on the age, a DOE reference pre-1980 construction set and a high infiltration rate per exterior surface area are assumed. The window to wall ratio is a visual estimation of the relative area of the windows in the building facade. As described in Chapter 4, I have assumed perimeter and core thermal zones at each floor with single space type. Closed office is selected as the space type for the whole building. Typical lighting and electric equipment are assumed for the loads. However, occupancy is not defined in the baseline model. Based on the visits it is assumed that the HVAC system is the DX cooling and district heating. The building is connected to the central steam distribution system of campus with steam pressure of 8.5 atm (125 psig). The building has a VAV system with reheat. The monthly end-use energy consumption is found below.

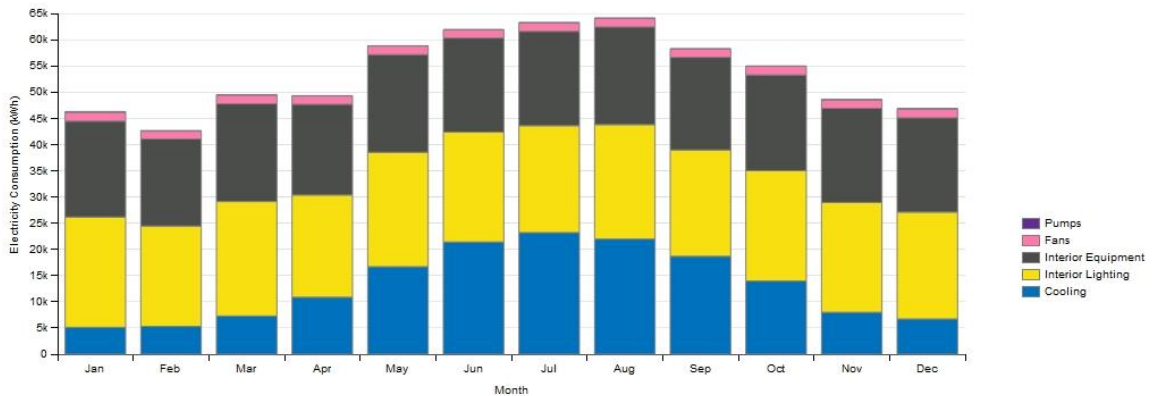


Figure 25: The monthly electricity consumption in the baseline energy model in 2014

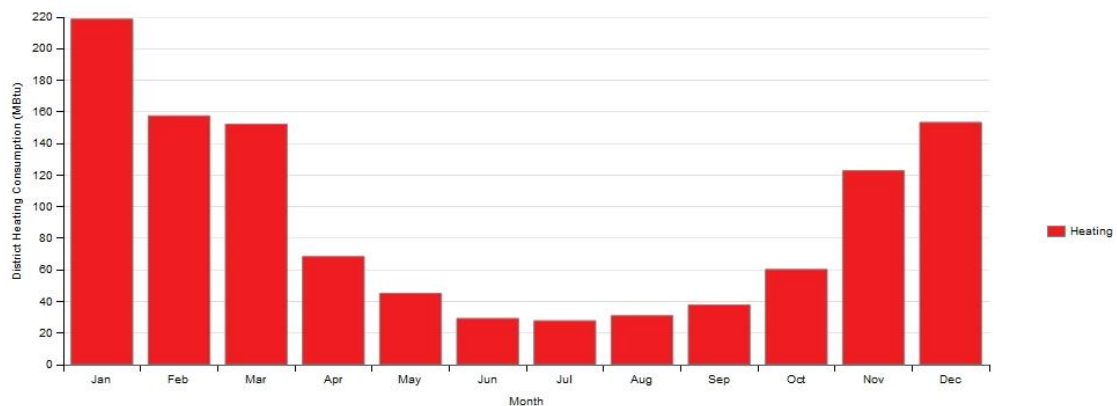


Figure 26: The monthly district steam consumption in the baseline energy model in 2014

The building is modeled to have the EUI of 1135 MJ/m<sup>2</sup> (100 kBtu/ft<sup>2</sup>). However, the metered data provided by the Facilities Management shows that the actual building EUI is 854 MJ/m<sup>2</sup> (75 kBtu/ft<sup>2</sup>) in 2014. The metered data which is shown in the next section is comprised by electricity and steam. The steam used by the building is assumed to be saturated vapor at 125 psig at the building entry and saturated liquid at atmospheric pressure for steam condensate at the outlet. The schedules with the changes applied are provided in the next section.

### *Section 6.3: Effect of Modified Weather Data on Specific Building Energy Use*

This section is about calibrating the energy model and investigating the effects of the modified weather data on the energy model. The reason that I use the weather data to calibrate the model is that we have to make sure the model is representing the building and then see the effects of different wind velocities in the calibrated energy model.

#### 6.3.1 Energy Model Calibration with Modified Weather Data

The baseline model and the actual building energy consumption were about 30% different. This difference necessitates calibrating the baseline model. In this thesis, the parameters suggested by National Renewable Energy Lab (NREL) revisited and modified in the OpenStudio energy model [61]. Based on this reference, there are common adjustments made during hand-calibration to monthly utility data. These parameters are categorized as primary, secondary, and tertiary based on their importance. Here I have worked on two years of monthly data of 2013 and 2014. The

primary parameters are ventilation and infiltration. The ventilation is not changed in the model as it is based on the values provided by ASHRAE 62.1 [62]. However, infiltration is the parameter that is changed drastically in the calibrated model. The baseline model uses the Design Flow Rate model from Eq.1. In that equation, there is a design flow rate  $I_{\text{design}}$  modified by a constant term, indoor-outdoor temperature difference, wind velocity, and wind velocity squared. In the baseline model the coefficients for constant, temperature, wind velocity, and wind velocity squared are 1,0,0,0, respectively. It means that the building sees a constant infiltration on the exterior surfaces. The calibrated model uses the coefficients from a study providing suitable coefficients for the Design Rate Flow model for different building types in EnergyPlus [36]. The coefficients used in the calibrated model are listed in Table 4. In addition to the infiltration adjustments, occupant definition and schedule changes are summarized below.

Table 4: The summary of the modifications in calibrating the energy model to monthly data

Calibration modification	Parameters
People	0.04 people/m <sup>2</sup> 0.3 fraction radiant 120 W/person, level of activity
Schedules	Shorter working hours based on heat maps Modified temperature setbacks
Infiltration	Design Flow Rate Model by medium office coefficients: 0.002 m <sup>3</sup> /m <sup>2</sup> s per exterior surface area (0.4 cfm/ft.min) Coefficients [36]: Constant term: 0.0 Temperature term: 0.0138 Wind velocity term: 0 Wind velocity squared term: 0.0315

The infiltration coefficients are for the infiltration at the time were the fans are off in medium office building, which is higher than the time when the fans are on and the building is pressurized. To correct the infiltration in the fan on period, an infiltration schedule is defined to have a quarter of the effect in the fan off mode. Occupancy schedules and temperature set points are some of the secondary parameters to adjust in calibration. The schedules are slightly changed. This change is mainly in temperature setbacks in unoccupied period. Using the heat maps for Mitchel building provided in Chapter 4, the working hour is squeezed shorter which reduces the heating and cooling loads. Moreover, the temperature setbacks are taken care of in the weekends. The summary of all the schedules are provided in Figure 28.

After applying the changes to the baseline model, the resulting EUI is 822.2 MJ/m<sup>2</sup> (72.4 kBtu/ft<sup>2</sup>), which is pretty close to the actual building 2014 EUI 854 MJ/m<sup>2</sup> (75.2 kBtu/ft<sup>2</sup>). The monthly electricity and steam consumption is illustrated in Figure 27. This figure shows that the baseline electricity was relatively close to the electricity data. However, the baseline steam was completely far off. Setting temperature setbacks, and mainly correcting infiltration led to a better monthly steam consumption in the calibrated model. The CVRMSE and NMBE, the two calibration indices from ASHRAE Guideline 14, are calculated in Table 5.

Table 5: Summary of the calibration indices

Utility	Index	Baseline model	Calibrated model
Electricity	CVRMSE	17%	9%
	NMBE	15%	0%
Steam	CVRMSE	168%	46% (14% heating)
	NMBE	108%	23% (1% heating)

The CVRME and NMBE need to be less than 15% and 5%, respectively, in the monthly calibration. The electricity is perfectly calibrated. However, steam is not completely calibrated. By looking at Figure 27, we see that main problem with steam is at summer months. While there is almost close to zero steam consumption in 2013, there is winter-like consumption in summer 2014. The problem might be because of a special operating or problems in metering.

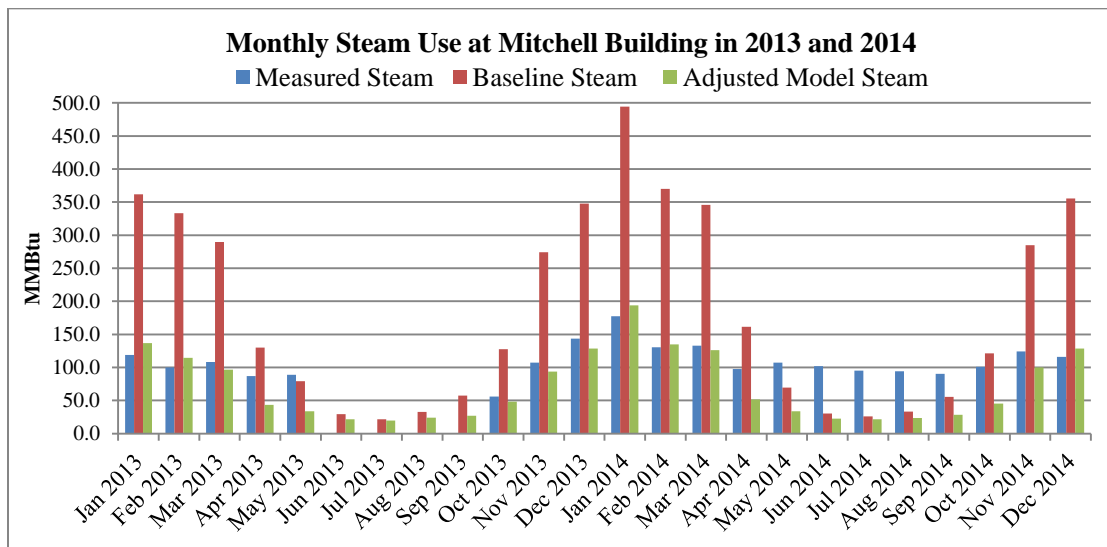
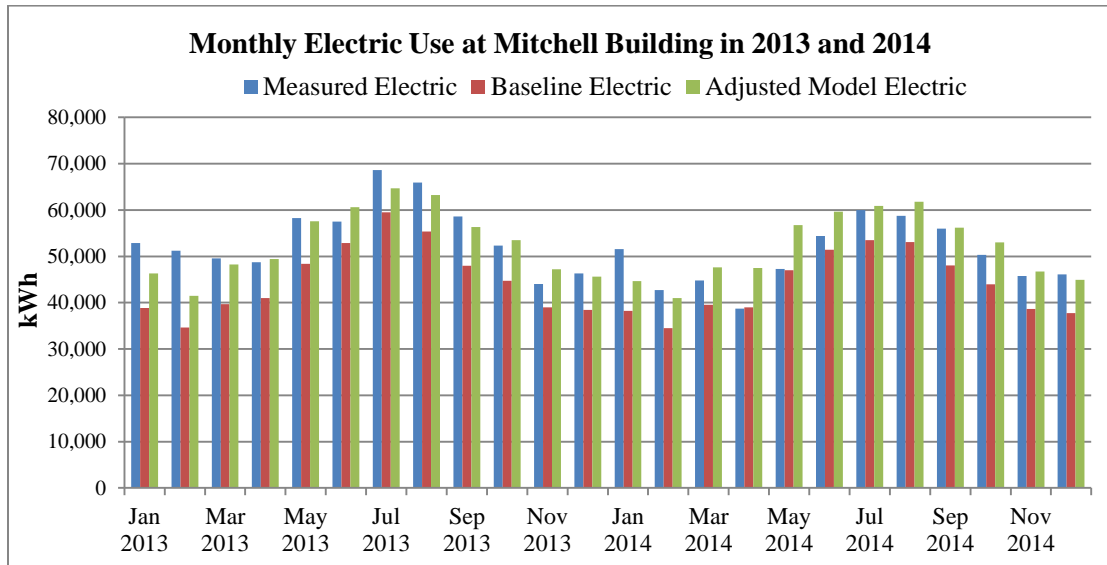


Figure 27: The measured, baseline, and calibrated monthly electricity and steam comparison



Metering steam at high pressures often comes with various difficulties. Usually the steam meters have a floor that registers the value passed them. In summer months, if the floor is set too high, they can register much less value that has passed through. This is a common problem with steam meters on central steam systems. With all these given, I have considered the heating months only to calculate another CVRMSE and NMBE for heating months. The heating months is assumed to be from November to April. The result shows that the CVRMSE and NMBE become 14% and 1%, respectively, if we only consider heating months.

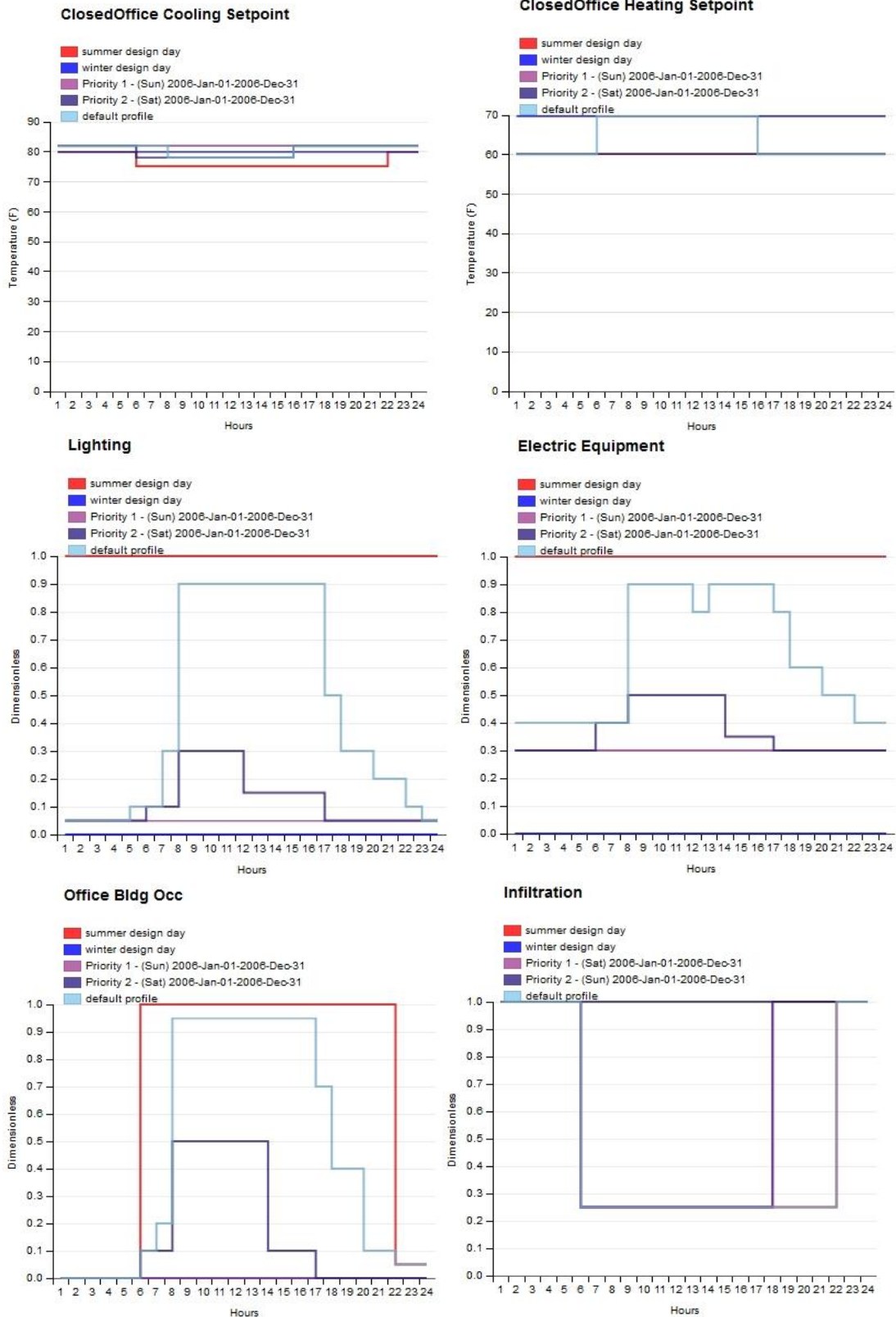


Figure 28: The schedules in the calibrated energy model, the “priority schedules” are used on weekends in 2014. The 2006 is the default year in OpenStudio to define the schedule.

### 6.3.2 Building Energy Use Comparison with Modified Weather Data

In this thesis, a baseline energy model was provided and then calibrated by adjusting the main important input parameters. The energy model now represents Mitchell building accurately, so we are capable of testing the influence of specific parameters. Based on the section 6.1, an adjusted weather data file is in hand. This weather data file has adjusted wind velocities for all the hours of an actual year.

Using the adjusted AMY 2014 weather file for College Park, MD brings about the EUI of  $822.2 \text{ MJ/m}^2$  ( $72.4 \text{ kBtu/ft}^2$ ). With the original unadjusted weather file, the EUI would be  $890.3 \text{ MJ/m}^2$  ( $78.4 \text{ kBtu/ft}^2$ ). The adjusted weather data caused a decrease of more than 5% in the total EUI of the building. Although this percentage is not very big, it is not unexpected. As described in the literature review, infiltration is responsible for 13% of the heating loads and 3% of the cooling loads for the US office buildings. Moreover, we knew that infiltration is the main parameter that aims to be influenced.

One important point about this wind effect is that even the 5% impact on EUI can be the difference between a calibrated vs. an uncalibrated model. Hence, the wind velocity aims to be influential in calibrating the models. In fact, wind velocity is not one of the main parameters in creating an energy model. However, it is to some extent influential on the energy model calibration.

To elaborate this point, there is the annual heat gains summary of the whole Mitchell building in 2014 in Figure 29. The figure shows the heat rejection or the heat removal in different categories with the adjusted and unadjusted weather data. I have to mention that as the figure illustrate the heat gain and heat losses, the total amount

of all the heat gains, equals the total amount of all the heat losses. It is clear that equipment, people and lighting are only heat additions that are not a function of this change. The reason is that they are defined based on the area and they are actually not physically related to weather. As the wind velocity is changed in the adjusted weather, it has changed the convective heat transfer coefficients, too. As a result, the heat removal through conduction and windows are reduced with the adjusted weather data. The most important point is that the heat removal and heat rejection by infiltration is reduced drastically. This decrease in infiltration contribution is more visible in the heat removal. Both heat removal and heat addition can happen any time of the year. Infiltration heat removal can occur in heating months and also in the early evenings or early mornings in summer months when the outside air gets colder than the indoor.

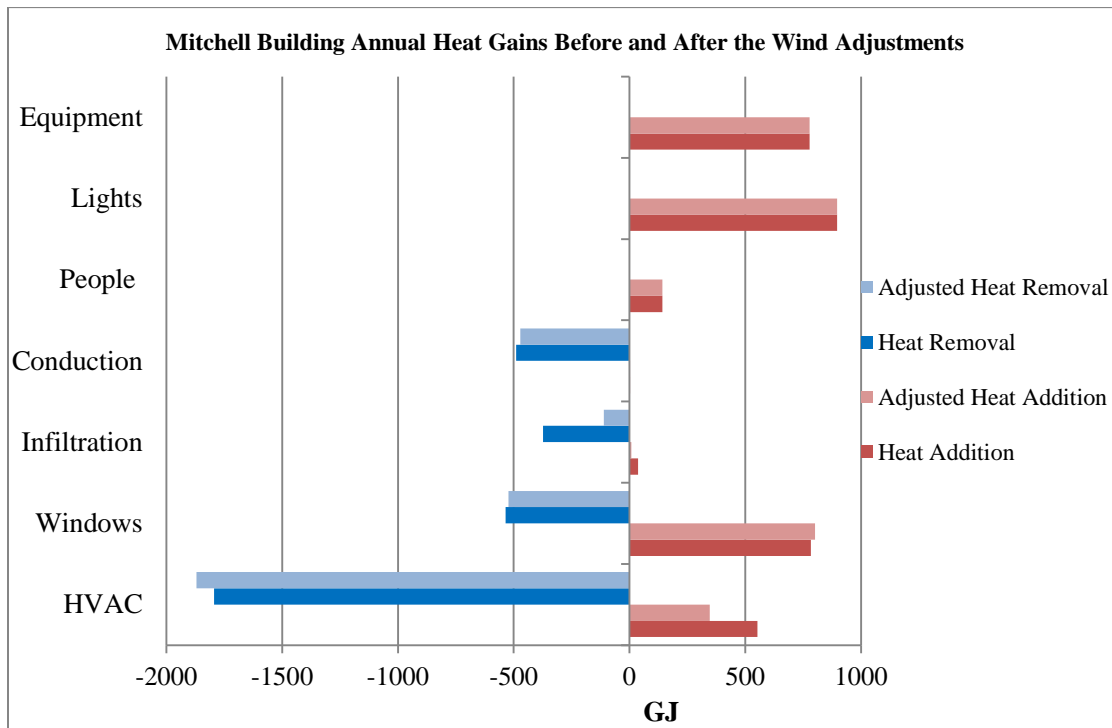


Figure 29: Annual heat gains for Mitchell building in 2014 by adjusted and original weather data

By this point, we have seen that the adjusted weather data has resulted in less heat removal from the building surfaces. Largely, it has resulted in reduction of heat removal by infiltration. To add up, there is less heat removal by the building envelope, which results in less HVAC heating. In other word, lower wind velocity in the wind neighborhood results in less surface heat transfer and mainly less infiltration for the building. This is a positive point in the building energy consumption during the heating mode. There is a 37% decrease in the total HVAC heat addition annually.

In the other side, the cooling loads such as equipment and lights are not changed much. In addition, heat removal mechanisms, especially infiltration, act weaker. The result is that there is 4% increase in the HVAC heat removal annually. This means that the cooling system needs to work harder during the summer months relative to what was expected.

We have to have it in mind that this effect can be lower in the air tight buildings as the outside is less infiltrating to the building. Moreover, we have to remember one of the main simplifying assumptions in this framework. This section generalized the wind multipliers for all of the incoming wind velocities in the weather data, although we calculated them based on the 1 m/s incoming wind.

In summary, although the adjusted wind velocities did not have a very significant impact on the total building EUI, it had considerable impact on the HVAC cooling and heating gain.

## Chapter 7: Conclusions

The literature review revealed that although considerable studies have considered modeling energy and airflow in built environment, there is a practical knowledge gap in considering neighborhood effects in building energy simulation programs. Researchers have used energy simulation and CFD programs to accurately predict local surface and air temperatures, convective heat transfer coefficients, and operational HVAC COPs in urban neighborhoods. However, the impact of local wind flow on the building energy consumption is along one of the parameters that are less considered in modeling buildings energy simulation.

The three objectives in the research study were to (1) develop a framework to quantify the impact of local wind flow in urban neighborhoods using airflow modeling in OpenFOAM CFD software and EnergyPlus energy simulation, (2) validate the CFD study with on-site temperature measurements in a campus neighborhood at the University of Maryland, and (3) calibrate the target building energy model with utilities data and use the energy model in comparing the adjusted weather data with local wind velocities.

The framework consists of modeling the airflow in the neighborhood where the wind blows from eight main principal directions. Measuring the local wind encountering the target building brings about wind multipliers in the eight principal directions. The wind multipliers adjust the wind speed in weather data, which is an input to the building energy model. The local wind influences on the building energy model through the adjusted weather data.

### Section 7.1: Thesis Conclusions

Conclusions from the present work are as follows:

1. In modeling airflow in urban neighborhoods using CFD, the method of meshing is one of the main important steps. Defining multiple boxes of mesh refinement in the size of the domain, secondary and primary buildings leads to sufficient level of mesh quality around primary (target) building with  $y^+$  value less than 300. The method in which we refine the mesh around the target building is of the main concern to reach required  $y^+$  value level.
2. Based on the validation of the CFD model with the on-site temperature measurements, using RNG k- $\epsilon$  turbulence model leads to more accurate prediction of the outdoor thermal environment rather than the Realizable k- $\epsilon$ . In the validation case, using the RNG k- $\epsilon$  model improved the CVRMSE from 6% to 2% in comparing CFD results with temperature measurements. In this study, ignoring the greeneries were the main source of the error in prediction of the air and surface temperature
3. Reduced-order energy modeling is efficient and useful in creating a baseline for building energy consumption. Moreover, heat maps of the utilities data are upon the best tools to improve the energy model with the actual building energy consumption.
4. Based on the case study, adjusting the weather data with the local wind in the urban neighborhood reduces the infiltration heat removal by 70%, decreases HVAC heating gain by 37%, and increases the HVAC cooling gain by 4% annually in the energy model.

### Section 7.2: Directions for Future Work

There are certain paths to improve this study with the final goal of fully understanding the urban thermal environment. First of all, one of the parameters that can be seen along with the local wind is the local temperature. Local temperature is usually dependent on a scale larger than a neighborhood. Developing a method to accurately representing a city-scale air temperature can greatly improve the results of this study. Second, implementing the proposed framework on various neighborhoods sheds more light on the actual physical phenomena in the urban thermal environment. Third, connecting the CFD and energy models in more communicative manner, transferring surface temperatures and local wind speeds can help to better model the neighborhood.



## Appendix A: OpenFOAM Validation Case Files

### **controlDict**

```
libs (
    "libOpenFOAM.so"
    "libsimpleSwakFunctionObjects.so"
    "libswakFunctionObjects.so"
    "libgroovyBC.so"
);
application    buoyantBoussinesqSimpleFoam;
startFrom      latestTime;
startTime      0;
stopAt         endTime;
endTime        10000;
deltaT         1;
writeControl   timeStep;
writeInterval  1000;
purgeWrite     0;
writeFormat    ascii;
writePrecision 7;
writeCompression off;
timeFormat     general;
timePrecision  6;
runTimeModifiable true;
```

## fvSchemes

```
ddtSchemes
{
    default    steadyState;
}

gradSchemes
{
    default    Gauss linear;
}

divSchemes
{
    default    none;
    div(phi,U)    bounded Gauss upwind cellLimited leastSquares 1.0;
    div(phi,T)    bounded Gauss upwind cellLimited leastSquares 1.0;
    div(phi,k)    bounded Gauss upwind cellLimited leastSquares 1.0;
    div(phi,epsilon) bounded Gauss upwind cellLimited leastSquares 1.0;
    div((nuEff*dev(T(grad(U)))))) Gauss linear;
}

laplacianSchemes
{
    default    none;
    laplacian(nuEff,U) Gauss linear corrected;
    laplacian((1|A(U)),p_rgh) Gauss linear corrected;
    laplacian((1|A(U)),p) Gauss linear corrected;
        laplacian(1,p)    Gauss linear corrected;
    laplacian(alphaEff,T) Gauss linear corrected;
    laplacian(DkEff,k) Gauss linear corrected;
    laplacian(DepsilonEff,epsilon) Gauss linear corrected;
    laplacian(DREff,R) Gauss linear corrected;
    laplacian(Dp,p_rgh) Gauss linear corrected;
}

interpolationSchemes
{
    default    linear;
}

snGradSchemes
{
    default    corrected;
}

fluxRequired
{
    default    no;
    p_rgh    ;
        p;
}
}
```

## fvSolution

```
solvers
{
  p_rgh
  {
    solver      GAMG;
    tolerance   1e-7;
    relTol      0.1;
    smoother    GaussSeidel;
    nPreSweeps  0;
    nPostSweeps 2;
    cacheAgglomeration on;
    agglomerator  faceAreaPair;
    nCellsInCoarsestLevel 10;
    mergeLevels  1;
  }
  "(U|T|k|epsilon|R)"
  {
    solver      smoothSolver;
    smoother    GaussSeidel;
    tolerance   1e-8;
    relTol      0.1;
    nSweeps     1;
  }
}
potentialFlow
{
  nNonOrthogonalCorrectors 8;
}
SIMPLE
{
  nNonOrthogonalCorrectors 1;
  pRefCell 0;
  pRefValue 0;

  residualControl
  {
    p_rgh 1e-4;
    U 1e-5;
    T 1e-5;

    // possibly check turbulence fields
    "(k|epsilon|omega)" 1e-5;
  }
}
relaxationFactors
{
  fields
  {
    p_rgh 0.2;
  }
  equations
  {
    U 0.3;
    T 0.3;
    "(k|epsilon|R)" 0.7;
  }
}
```

## Appendix B: MATLAB Code for Wind Multipliers

```
%Mitchell Building Case Study
%This code imports the AMY weather data in csv format
%looks at the wind direction column in degrees and
%multiplies the wind velocity with the corresponding wind
multiplier
%Inputs
WM_N = 0.63;
WM_NE = 0.74;
WM_E = 0.74;
WM_SE = 0.64;
WM_S = 0.40;
WM_SW = 0.59;
WM_W = 0.79;
WM_NW = 0.75;

%Initial weeather data import
data_csv= csvread('2013_amy_V1.csv');
data=data_csv;
%Identifying the wind direction range
%and multiplying the related wind multiplier
for n=1:8760
    if 0.00 <= data(n,20) && data(n,20) < 22.50
        data(n,21) = WM_N * data(n,21); %North wind multiplier
    elseif 22.50 <= data(n,20) && data(n,20) < 67.50
        data(n,21) = WM_NE * data(n,21); %Northeast wind
multiplier
    elseif 67.50 <= data(n,20) && data(n,20) < 112.50
        data(n,21) = WM_E * data(n,21); %East wind multiplier
    elseif 112.50 <= data(n,20) && data(n,20) < 157.50
        data(n,21) = WM_SE * data(n,21); %Southeast wind
multiplier
    elseif 157.50 <= data(n,20) && data(n,20) < 202.50
        data(n,21) = WM_S * data(n,21); %South wind multiplier
    elseif 202.50 <= data(n,20) && data(n,20) < 247.50
        data(n,21) = WM_SW * data(n,21); %Southwest wind
multiplier
    elseif 247.50 <= data(n,20) && data(n,20) < 292.50
        data(n,21) = WM_W * data(n,21); %West wind multiplier
    elseif 292.50 <= data(n,20) && data(n,20) < 337.50
        data(n,21) = WM_NW * data(n,21); %Northwest wind
multiplier
    elseif 337.50 <= data(n,20)
        data(n,21) = WM_N * data(n,21); %North wind multiplier
    else
        data(n,21)=99; % shows error
    end
end
end
% Writing the adjusted AMY weather data file
csvwrite('2013amy_V2.csv',data);
```

## Bibliography

- [1] B. Cohen, "Urbanization in developing countries: Current trends, future projections, and key challenges for sustainability," *Technology in Society*, pp. 63-80, 2006.
- [2] United Nations, "World Urbanization Prospects," 2014.
- [3] US Energy Information Administration, "Future world energy demand driven by trends in developing countries," 3 December 2013. [Online]. Available: <http://www.eia.gov/todayinenergy/detail.cfm?id=14011>.
- [4] Department of Energy, "Buildings Energy Data Book," March 2012. [Online]. Available: <http://buildingsdatabook.eren.doe.gov/TableView.aspx?table=1.1.3>.
- [5] J. Srebric, M. Heidarinejad and J. Liu, "Building neighborhood emerging properties and their impacts on multi-scale modeling of building energy and airflows," *Building and Environment*, pp. 242-262, 2015.
- [6] Y. Toparlar, B. Blocken, P. Vos, G. van Heijst, W. Janssen, T. van Hooff, H. Montazeri and H. Timmermans, "CFD simulation and validation of urban microclimate: A case study for Bergpolder Zuid, Rotterdam," *Building and Environment*, pp. 79-90, 2015.
- [7] X. Yang, L. Zhao, M. Bruse and Q. Meng, "An integrated simulation method for building energy performance assessment in urban environments," *Energy and Buildings*, pp. 243-251, 2012.
- [8] N. Yaghoobian and J. Kleissl, "An indoor-outdoor building energy simulator to study urban modification effects on building energy use - Model description and validation," *Energy and Buildings*, pp. 407-417, 2012.
- [9] B. Bueno, L. Norford and G. Pigeon, "Combining a detailed building energy model with a physically-based urban canopy model," *Boundary-Layer Meteorology*, pp. 471-489, 2011.
- [10] J. Bouyer, C. Inard and M. Musy, "Microclimatic coupling as a solution to improve building energy simulation in an urban context," *Energy and Buildings*, pp. 1549-1559, 2011.
- [11] J. Liu, M. Heidarinejad, S. Gracik, J. Srebric and N. Yu, "An indirect validation of convective heat transfer coefficients (CHTCs) for external building surfaces in an actual urban environment," *Building Simulation*, pp. 337-352,

2015.

- [12] J. Liu, M. Heidarinejad, S. Gracik and J. Srebric, "The impact of exterior surface convective heat transfer coefficients on the building energy consumption in urban neighborhoods with different plan area densities," *Energy and Buildings*, pp. 449-463, 2015.
- [13] J. L. Santiago, F. Martin and A. Martilli, "A computational fluid dynamic modeling approach to assess the representativeness of urban monitoring stations," *Science of the Total Environment*, pp. 61-72, 2013.
- [14] M. Neophytou, A. Gowardhan and M. Brown, "An inter-comparison of three urban wind models using Oklahoma City Joint Urban 2003 wind field measurements," *Journal of Wind Engineering and Industrial Aerodynamics*, pp. 357-368, 2011.
- [15] B. Blocken, J. Carmeliet and T. Stathopoulos, "CFD evaluation of wind speed conditions in passages between parallel buildings-effect of wall function roughness modifications for the atmospheric boundary layer flow," *Journal of Wind Engineering and Industrial Aerodynamics*, pp. 941-962, 2007.
- [16] B. Blocken, T. Stathopoulos and J. Carmeliet, "CFD simulation of the atmospheric boundary layer: wall function problems," *Atmospheric Environment*, pp. 238-252, 2007.
- [17] J. Allegrini, V. Dorer and J. Carmeliet, "Coupled CFD, radiation and building energy model for studying heat fluxes in an urban environment with generic building configurations," *Sustainable Cities and Society*, pp. 385-384, 2015.
- [18] C. Gromke, B. Blocken, W. Janssen, B. Merema, T. van Hooff and H. Timmermans, "CFD analysis of transpirational cooling by vegetation: Case study for specific meteorological conditions during a heat wave in Arnhem, Netherlands," *Building and Environment*, pp. 11-26, 2015.
- [19] R. Zhang, K. P. Lam, S.-c. Yao and Y. Zhang, "Coupled EnergyPlus and computational fluid dynamics simulation for natural ventilation," *Building and Environment*, pp. 100-113, 2013.
- [20] S. Somarathne, M. Seymour and M. Kolokotroni, "Dynamic thermal CFD simulation of a typical office by efficient transient solution methods," *Building and Environment*, pp. 887-896, 2005.
- [21] S. Gracik, M. Heidarinejad, J. Liu and J. Srebric, "Effect of urban neighborhoods on the performance of building cooling systems," *Building and Environment*, pp.

15-29, 2015.

- [22] S. Gracik, "The effect of urban density on building HVAC performance, MS Thesis," Pennsylvania State University, 2014.
- [23] J. Franke, A. Hellsten, H. Schlunzen and B. Carissimo, "The Best Practise Guideline for the CFD simulation of flows in the urban environment: an outcome of COST 732," in *International Symposium on Computational Wind Engineering*, Chapel Hill, North Carolina, USA, 2010.
- [24] Z. Zhai, Q. Chen, P. Haves and J. Klems, "On approaches to couple energy simulation and computational fluid dynamics programs," *Building and Environment*, pp. 857-864, 2002.
- [25] A. Novoselac, Combined airflow and energy simulation program for building mechanical system design, Doctoral Thesis, Pennsylvania State University, 2005.
- [26] I. Beausoleil-Morrison, J. Clarke, J. Denev, I. MacDonald, A. Melikov and P. Stankov, "Integrating CFD and building simulation," *Building and Environment*, pp. 865-871, 2002.
- [27] Z. Zhai and Q. Chen, "Performance of coupled building energy and CFD simulations," *Energy and Buildings*, pp. 333-344, 2005.
- [28] C. Peng and A. Elwan, "An outdoor-indoor coupled simulation framework for climate change-conscious urban neighborhood design," *Transactions of the Society for Modeling and Simulation International*, pp. 1-18, 2014.
- [29] M. Taleghani, L. Kleerekoper, M. Tenpierik and A. van den Dobbela, "Outdoor thermal comfort within five different urban forms in the Netherlands," *Building and Environment*, pp. 65-78, 2015.
- [30] G. H. Han, J. Srebric and E. Enache-Pommer, "Different modeling strategies of infiltration rates for an office building to improve accuracy of building energy simulations," *Energy and Buildings*, pp. 288-295, 2015.
- [31] M. Liddament and M. Orme, "Energy and ventilation," *Applied Thermal Engineering*, pp. 1101-1109, 1998.
- [32] M. Sherman, Air infiltration in buildings, PHD thesis, 1980.
- [33] S. Emmerich and A. Persily, "Energy impacts of infiltration and ventilation in US office buildings using multizone airflow simulation," in *Proceedings of IAQ*

*and Energy, Vol.98, 1998.*

- [34] EnergyPlus Engineering Reference, 2014.
- [35] C. Coblenz and P. Achenbach, "Field measurement of ten electrically-heated houses," in *ASHRAE Transactions*, 1963.
- [36] L. C. Ng, A. Persily and S. J. Emmerich, "Improving infiltration modeling in commercial building energy models," *Energy and Buildings*, pp. 316-323, 2015.
- [37] M. Sherman and D. Grimsurd, "Infiltration-pressurization correlation: Simplified physical modeling," in *ASHRAE Transactions*, 1980.
- [38] I. Walker and D. Wilson, "Field validation of equations for stack and wind driven air infiltration calculations," *International Journal of HVAC&R Research*, 1998.
- [39] b. Burley, "Infiltration mapping for urban environments," Pennsylvania State University, 2009.
- [40] OpenFOAM Licensing, 2016. [Online]. Available: <http://www.openfoam.com/legal/open-source.php>.
- [41] M. Pitman and C. Watts, "A building simulation tool for the rapid feedback of scientific data in architectural design," in *45th Annual Conference of the Architectural Science Association*, Sydney, 2011.
- [42] EnergyPlus Licensing, 2016. [Online]. Available: <https://energyplus.net/licensing>.
- [43] J. Srebric, "Simplified Methodology for Indoor Environment Design," Massachusetts Institute of Technology, 2000.
- [44] M. Heidarinejad, N. Mattise, M. Dahlhausen, S. Khoshdel Nikkho, J. Liu, S. Gracik, K. Liu, S. Krishang, H. Zhang, J. Wentz, M. Sadeghipour Roudsari, G. Pitchurov and J. Srebric, "Urban scale modeling of campus building using Virtual PULSE," in *International Building Performance Simulation Association (IBPSA)*, Hyderabad, India, 2015.
- [45] ASHRAE Guideline 14, "Measurement of Energy and Demand Savings," 2002. [Online]. Available: [https://gaia.lbl.gov/people/ryin/public/Ashrae\\_guideline14-2002\\_Measurement%20of%20Energy%20and%20Demand%20Saving%20.pdf](https://gaia.lbl.gov/people/ryin/public/Ashrae_guideline14-2002_Measurement%20of%20Energy%20and%20Demand%20Saving%20.pdf).



- [46] M. Heidarinejad, M. Dahlhausen, N. Mattise, K. Sharma, K. Benne, D. Macumber and J. Srebric, "Demonstration of reduced-order urban scale building energy simulations," *Applied Energy*, 2016.
- [47] M. Heidarinejad, "Relative significance of heat transfer processes to quantify tradeoffs between complexity and accuracy of energy simulations with a building energy use patterns classification," Pennsylvania State University, 2014.
- [48] "OpenFOAM C++ Documentation," 2014. [Online].
- [49] J. Ferziger and M. Peric, *Computational Methods for Fluid Dynamics*, Berlin: Springer-Verlag, 2002.
- [50] W. Kays and M. Crawford, *Convective Heat and Mass Transfer*, New York: McGraw-Hill, Inc., 1993.
- [51] OpenFOAM, *The Open Source CFD Toolbox User Guide*, 2014.
- [52] B. Martinez, "Wind resource in complex terrain with OpenFOAM," Technical University of Denmark, 2011.
- [53] J. Franke, A. Hellsten, H. Schlünzen and B. Carissimo, "Best practice guideline for the CFD simulation of flows in the urban environment," *COST action*, p. 51, 2007.
- [54] J. Liu, J. Srebric and N. Yu, "A Rapid and Reliable Numerical Method for Predictions of Outdoor Thermal Environment in Actual Urban Areas," in *ASME 2013 Heat Transfer Summer Conference collocated with the ASME 2013 7th International Conference on Energy Sustainability and the ASME 2013 11th International Conference on Fuel Cell Science, Engineering and Technology*, Minneapolis, Minnesota, 2013.
- [55] "EnergyPlus Engineering Reference," 2013.
- [56] A. Rakai and G. Kristóf, "CFD simulation of flow over a mock urban setting," in *5th OpenFOAM workshop*, Chalmers, Sweden, 2010.
- [57] Y. Miao, S. Liu, B. Chen, B. Zhang, S. Wang and S. Li, "Simulating urban flow and dispersion in Beijing by coupling a CFD model with the WRF model," *Advances in Atmospheric Sciences*, pp. 1663-1678, 2013.
- [58] A. Jackson, E. de Villiers, F. Campos, M. Beyers, J. Kastrup and J. C. Bennetsen, "Prediction of pedestrian wind and thermal comfort and pollutant dispersal in an urban environment," in *6th OpenFOAM Workshop*, University Park, Pennsylvania, 2011.

- [59] D. Hargreaves and N. Wright, "On the use of the k-epsilon model in commercial CFD software to model the neutral atmospheric boundary layer," *Journal of Wind Engineering and Industrial Aerodynamics* , pp. 355-369, 2007.
- [60] F. M. White, *Viscous Fluid Flow*, McGraw-Hill, 1991.
- [61] E. Hale, L. Lisell, D. Goldwasser, D. Macumber, J. Dean, I. Metzger, A. Parker, N. Long, B. Ball, M. Schott, E. Weaver and L. Brackney, "Cloud-based model calibration using OpenStudio," in *eSim 2014*, Ottawa, Canada, 2014.
- [62] ASHRAE Standard 62.1, "Ventilation for Acceptable Indoor Air Quality," 2013.